



## MASTER THESIS

Neurological outcome prediction of comatose patients after cardiac arrest based on EEG, brain MRI and optic nerve ultrasonography

M.M.L.H. Verhulst  
Technical Medicine

March 2020



UNIVERSITY OF TWENTE.



# NEUROLOGICAL OUTCOME PREDICTION OF COMATOSE PATIENTS AFTER CARDIAC ARREST BASED ON EEG, BRAIN MRI AND OPTIC NERVE ULTRASONOGRAPHY

## AUTHOR

M.M.L.H. Verhulst

*Graduate student Technical Medicine*

*Medical Sensing and Stimulation track*

*Clinical specialization internship at Rijnstate hospital Arnhem*

*Department of neurology*

## EXAMINATION COMMITTEE

Chair & technological supervisor	Prof. dr. ir. M.J.A.M. van Putten
Medical supervisor	Prof. dr. J. Hofmeijer
Daily supervisor	H.M. Keijzer, MSc.
Process supervisor	Drs. P.A. van Katwijk
External member	Prof. dr. ir. B. ten Haken

## COLLOQUIUM

Date	March 11, 2020
Time	11 AM
Place	Technohal (TL) 1133, University of Twente



## ABSTRACT

**Introduction** Postanoxic encephalopathy is the main cause of death in the hospital after cardiac arrest. Early prediction of neurological outcome is important for families and treating physicians. Prediction is nowadays based on neurological examination, somatosensory evoked potentials (SSEPs) and the EEG. These measures can identify approximately half of all patients with poor neurological outcome. Quantitative and qualitative MRI measures and ultrasonographic measurement of the optic nerve sheath diameter (ONSD) have been suggested to add to neurological outcome prediction after cardiac arrest.

**Objectives** To investigate the additional value of MRI measures, in addition to the EEG, to predict neurological outcome of comatose patients after cardiac arrest and to estimate the feasibility and potential value of repetitive ONSD measurements to further improve outcome prediction.

**Methods** We included comatose patients after cardiac arrest. Continuous EEG was measured during the first 3 days. EEGs were classified as unfavourable, favourable or intermediate based on visual and quantitative classification. MRI scans were performed at day 2-4 after cardiac arrest. FLAIR, DWI and SWI scans were visually scored by two neuroradiologists. ADC maps were quantitatively assessed. Ultrasonographic measurements of the ONSD were performed at day 1-3 after cardiac arrest. MRI, EEG and ONSD measures were related to neurological outcome. Analyses of diagnostic value for good or poor outcome were based on receiver operating characteristics and calculation of sensitivity and specificity.

**Results** In the MRI study we included 30 patients, of whom 14 had poor neurological outcome. Most promising visual MRI parameters for prediction of good or poor neurological outcome were the Cortex score and DGN score, respectively. Most promising quantitative MRI measure to predict both good and poor outcome was the proportion of brain volume with an ADC value below  $450 \times 10^{-6} \text{ mm}^2/\text{s}$ . Visual and quantitative EEG measures could identify 21% of all patients with poor neurological outcome. Adding visual and quantitative MRI measures, increased sensitivity for prediction of poor neurological outcome to 86% at 100% specificity. In the ONSD study we included 11 patients, of whom 6 had poor neurological outcome. No significant differences of the ONSD between patients with good and poor neurological outcome were found at day 1 and 2 after cardiac arrest. At day 3, patients with poor neurological outcome had significant lower ONSD measurements than patients with good neurological outcome. No significant differences in trends over time between patients with good and poor neurological outcome were found.

**Conclusion** Visual and quantitative analysis of brain DWI and FLAIR MRI performed on day 2-4 after cardiac arrest hold potential to increase sensitivity for prediction of good or poor neurological outcome, with equal reliability. We could not replicate previously described predictive values of ultrasonographic measurements of the ONSD, yet.



## LIST OF ABBREVIATIONS

ADC	apparent diffusion coefficient
BCI	background continuity index
BOLD	blood oxygenation level dependent
BSAR	burst suppression amplitude ratio
CPC	cerebral performance category
CSF	cerebrospinal fluid
DGN	deep grey nuclei
DMVs	deep medullary veins
DTI	diffusion tensor imaging
DWI	diffusion weighted imaging
EEG	electroencephalogram
EPSP	excitatory postsynaptic potentials
fMRI	functional MRI
FLAIR	fluid attenuated inversion recovery
FPR	false positive rate
GCS	Glasgow coma scale
GPD	generalized periodic discharge
ICP	intracranial pressure
ICU	intensive care unit
IPSP	inhibitory postsynaptic potentials
IQR	interquartile range
MRI	magnetic resonance imaging
NSE	neuron specific enolase
ONSD	optic nerve sheath diameter
ROC	receiver operating characteristic
ROSC	return of spontaneous circulation
SSEP	somatosensory evoked potential
SWI	susceptibility weighted imaging



# TABLE OF CONTENTS

Chapter 1 Introduction .....	7
Chapter 2 Neurological outcome prediction based on EEG and MRI .....	9
2.1 Methods .....	9
2.2 Results .....	16
2.3 Discussion .....	25
2.4 Conclusion .....	28
Chapter 3 Neurological outcome prediction based on ultrasound .....	31
3.1 Methods .....	31
3.2 Results .....	33
3.3 Discussion .....	35
3.4 Conclusion .....	37
Chapter 4 General conclusion and future directions .....	39
Future directions .....	39
Conclusion .....	40
Bibliography .....	41
Appendices .....	45
Appendix A - General background .....	45
Appendix B – EEG analyses.....	53
Appendix C – Visual FLAIR and DWI analysis .....	54
Appendix D – Visual SWI analysis .....	55
Appendix E – Quantitative MRI analysis .....	56
Appendix F – Correlation between EEG and MRI .....	57
Appendix G – Trends of ONSD .....	58



# CHAPTER 1

## INTRODUCTION

Cardiac arrest has an incidence of 50-110 per 100,000 people a year worldwide, making it a leading cause of death in western countries [1]. Most patients initially surviving cardiac arrest remain comatose after return of spontaneous circulation (ROSC) for an insecure amount of time. Of these comatose patients, 40 to 60% never regain consciousness due to permanent brain damage [2-4] and only 10 to 20% of all cardiac arrest patients survive to hospital discharge [5, 6]. Postanoxic encephalopathy is the main cause of death in the hospital [7, 8].

Early prediction of neurological outcome of comatose patients after cardiac arrest is of great importance for patients' families, as well as treating physicians. Identification of patients without potential for recovery of brain function may help physicians and patients' families in making an informed decision regarding withdrawal of treatment [5].

Reliable prediction of a poor neurological outcome and subsequent withdrawal of treatment is nowadays based on a combination of neurological examination, somatosensory evoked potentials (SSEP) and the EEG in the first 24 hours after cardiac arrest [9]. These examinations allow reliable identification of approximately half of all patients that will have a poor outcome, with a reported false positive rate of 0% [2, 10-13]. Nevertheless, neurological outcome of the other 75% of all patients remains uncertain. Therefore, many patients are treated on intensive care units (ICUs) with unknown recovery perspectives.

Over the past years, various studies have provided additional measures for neurological outcome prediction of comatose postanoxic patients. Quantitative and qualitative electroencephalography (EEG) measures and brain imaging were investigated in particular. EEG studies have shown that both visual classification of the EEG and quantitative EEG measures can predict either good or poor neurological outcome in up to 50% of all comatose patients [2, 12-15]. Magnetic resonance imaging (MRI) studies have shown significant differences in brain structure between patients with good and poor neurological outcome. These differences could be detected with either visual or quantitative analysis of MRI data [16-24]. However, predictive values of MRI measures are unclear and studies combining EEG and MRI are scarce.

Three studies investigated added value of MRI measures on EEG patterns for neurological outcome prediction [25-27]. These studies showed that quantitative MRI measures (whole brain apparent diffusion coefficient (ADC) and proportion of brain with ADC values below certain thresholds) or visual MRI analysis could add to visual classification of the EEG for neurological outcome prediction of comatose patients after cardiac arrest. However, no research was found that combined both quantitative and visual EEG measures and quantitative and visual MRI features to improve the prediction of neurological outcome in comatose patients after cardiac arrest.

Apart from EEG and brain imaging, the optic nerve sheath diameter (ONSD) has been investigated for prognosis of neurological outcome after cardiac arrest. Raised intracranial pressure (ICP), resulting from ischemic brain oedema, is expected to contribute to poor neurological outcome [28-30]. However,

invasive ICP measurements are risky and may cause additional brain damage. Various studies have suggested that ultrasonographic measurements of the ONSD provide information about ICP [31-33] and that an increased ONSD can be predictive for poor neurological outcome [28-30]. However, the optimal timing to perform ONSD measurements is unknown and the utility of repeated measurements has not been clarified. Furthermore, no threshold has been found yet to discriminate a 100% in hospital mortality rate.

In chapter 2 of this thesis, we will investigate the additional value of MRI measures, in addition to the EEG, to predict neurological outcome of comatose patients after cardiac arrest. Also, we will employ combined EEG and MRI measurements to gain insight in the association between pathological EEG patterns and structural brain lesions on the brain MRI.

In chapter 3, we will estimate the feasibility and potential value of repetitive ultrasonographic measurements of the ONSD to further improve outcome prediction. In chapter 4 we present general conclusions and propose future directions.

## CHAPTER 2

### NEUROLOGICAL OUTCOME PREDICTION BASED ON EEG AND MRI

#### RESEARCH QUESTIONS

What is the additional value of structural brain abnormalities on diffusion weighted imaging (DWI) and fluid attenuated inversion recovery (FLAIR) images on day 2-4 after resuscitation, in addition to previously defined electroencephalography (EEG) measures, for neurological outcome prediction of comatose patients after cardiac arrest?

- What is the predictive value of visual and quantitative brain MRI analysis for good or poor neurological outcome?
- What is the association between EEG and MRI measures?

#### 2.1 METHODS

##### 2.1.1 Study Design

This is a prospective cohort study on EEG and magnetic resonance imaging (MRI) based outcome prediction of adult comatose patients after cardiac arrest, conducted on the intensive care unit (ICU) of Rijnstate Hospital (Arnhem) and Radboudumc (Nijmegen). The study was approved by the Committee on Research Involving Human Subjects region Arnhem-Nijmegen. Data for the current analyses were collected from June 2018 to February 2020.

##### 2.1.2 Study population

Legal representatives of consecutive adult patients after cardiac arrest with a presumed cardiac cause or pulmonary embolism, who were admitted comatose (Glasgow Coma Scale (GCS)  $\leq 8$ ) to the ICU of Rijnstate Hospital or Radboudumc, were asked for written informed consent within 72 hours after cardiac arrest. As soon as patients were mentally competent to make decisions, they were also asked for written deferred consent. Exclusion criteria were pregnancy, life expectancy  $< 24$  hours, any known progressive brain illness, such as a brain tumour or neurodegenerative disease, a known contra-indication for MRI, and pre-existing dependency in daily living (cerebral performance category (CPC) 3 or 4).

##### 2.1.3 Standard of care

Patients were monitored and treated according to guidelines for comatose cardiac arrest patients as described in local ICU protocols. Targeted temperature management at 36 °C (Rijnstate Hospital) or 32-34 °C (Radboudumc) was induced as soon as possible after arrival at the emergency room or ICU and maintained for 24 hours. After 24 hours, passive rewarming was controlled to a speed of 0.25 °C or 0.5 °C per hour. In Rijnstate, in case of a temperature  $> 38$  °C and a GCS score  $\leq 8$ , targeted temperature management was restarted at 36.5 °C to 37.5 °C for another 48 hours. In Radboudumc, temperature was kept below 38 °C for 5 days. Patients received a combination of propofol, midazolam, morphine, remifentanyl and/or sufentanyl for sedation.

### 2.1.4 Decisions on withdrawal of treatment

Withdrawal of treatment was considered at  $\geq 72$  hours after cardiac arrest, during normothermia, and off sedation. Decisions on withdrawal of treatment were based on national guidelines including incomplete return of brainstem reflexes, treatment-resistant myoclonus and bilateral absence of somatosensory evoked potentials (SSEPs) [9]. Neither the EEG within 72 hours nor any MRI measure was included in decisions of treatment withdrawal.

### 2.1.5 Data collection

#### *EEG*

Continuous EEG recordings were started as soon as possible after arrival at the ICU and were continued for three days or until patient awakening, as part of standard care in both hospitals. At Rijnstate Hospital twenty-one silver-silverchloride electrodes were placed on the scalp according to the international 10-20 system. A Nihon Kohden system (VCM Medical, The Netherlands) was used for continuous EEG registration. At Radboudumc ten silver-silverchloride electrodes were placed on the scalp according to the reduced montage described by Tjepkema-Cloostermans et al.[34] A NicoletOne (Natus Medical Incorporated, San Carlos, CA) was used for continuous EEG registration. All EEG analyses were prespecified and performed offline.

#### *MRI*

All patients underwent an MRI scan at day  $3 \pm 1$  days after cardiac arrest. The imaging protocol consisted of 3D T1, FLAIR, DWI, Susceptibility Weighted Imaging (SWI), Diffusion Tensor Imaging (DTI) and Blood Oxygenation Level Dependent functional MRI (BOLD fMRI) sequences. The current analysis included FLAIR (Rijnstate: TE=minimum, TR=4800ms, FA=40°, voxel size=1.12x1.12x1.12mm, Radboudumc: TE=294ms, TR=4800ms, FA=100°, voxel size=0.5x0.5x0.6mm), DWI (Rijnstate: TE=minimum, TR=minimum, FA=90°, voxel size=1.85x2.32x3mm, B value=1000, Radboudumc: TE=64ms, TR=6060ms, FA=180° voxel size=1x1x2mm, B value=1000) and SWI (Rijnstate: TE=minimum, TR=minimum, FA=10°, voxel size=1x1x1mm, Radboudumc: TE=21ms, TR=26ms, FA=10°, voxel size=0.5x0.5x0.5mm).

MRI imaging was performed using a 3 Tesla Philips Ingenia (Rijnstate) and Siemens Skyra (Radboudumc) system.

#### *Neurological outcome*

The primary outcome measure was neurological outcome expressed as the CPC score at six months after cardiac arrest. Outcome was dichotomized as “good” (CPC 1-2) or “poor” (CPC 3-5). CPC scores were assessed by a telephone interview by a trained investigator at six months. Scoring was based on a Dutch translation of the EuroQol-6D questionnaire.

### 2.1.6 Data analysis

#### *EEG pre-processing*

A computer algorithm selected 5-minute artefact-free EEG epochs at 6, 12, 24, 36, 48, and 72 hours after cardiac arrest and at the last available hour before MRI. Channels with muscle artefacts, high-

amplitude artefacts and flat channels were excluded by an artefact detection algorithm[13]. If at least two-third of the channels were artefact-free, the epoch was included in further analysis. If no artefact-free epoch was available at the selected time point, the closest available epoch in the range  $\pm 2$  hours was used. These EEG epochs were filtered with a sixth order zero-phase Butterworth bandpass filter with a frequency range of 0.5 to 35 Hz.

#### *Visual EEG classification*

Visual EEG classification was performed offline. All EEG epochs were presented to two independent reviewers by the computer, in random order. Reviewers were blinded to the point in time of the epoch, the patient's clinical status during the recording, medication, and neurological outcome. Upon disagreement, consensus was determined by consultation of a third reviewer.

Visual EEG classification was based on previous work of Ruijter et al.[14]. EEG patterns were classified as suppressed, synchronous with  $\geq 50\%$  suppression, continuous or other patterns (table 2.1). At 6, 12, 24, 36, 48, and 72 hours, each patient's EEG was classified as favourable, unfavourable or intermediate. Suppressed and synchronous activity with at least 50% suppressions were categorized as unfavourable patterns. Continuous activity was categorized as a favourable pattern and all other activity was categorized as intermediate.

Based on all available EEG scores, EEGs were classified as favourable (at least one continuous EEG pattern at 6 or 12 hours after cardiac arrest) or unfavourable (at least one unfavourable EEG pattern at 6, 12 or 24 hours after cardiac arrest) or intermediate (all other EEG scores) [14].

TABLE 2.1 OVERVIEW OF THE EEG CATEGORIES WITH CORRESPONDING EEG PATTERNS FOR VISUAL EEG CLASSIFICATION.

Category	Explanation
<b>Unfavourable</b>	<b>Suppressed</b> Suppressed (maximum amplitude < 10µV)
<b>Unfavourable</b>	<b>Synchronous with ≥ 50% suppressions*</b> Synchronous burst-suppression with generalized, abrupt-onset bursts or identical bursts with suppressed background activity Generalized periodic discharges with suppressed background activity
<b>Favourable</b>	<b>Continuous or nearly continuous activity: maximum amplitude ≥ 20µV, &lt; 10% suppressions*</b> Delta (dominant frequency < 4 Hz) Theta (dominant frequency 4-8 Hz) Alpha (dominant frequency > 8 Hz)
<b>Intermediate</b>	<b>Other patterns</b> Low-voltage (maximum amplitude 10-20 µV) Epileptiform on other background Burst-suppression (heterogeneous with ≥ 50% suppressions*) Discontinuous (10-49% suppressions*)

\* suppressions are defined as one of the following:

- Segments with amplitude < 10µV
- Segments with amplitude ≥ 10µV, but < 50% of background/burst voltage

### Quantitative EEG analysis

Background Continuity Index (BCI), burst suppression amplitude ratio (BSAR) and a model based on BCI and BSAR were used as quantitative EEG measures.[13]

The BCI is a measure for the continuity of the EEG and could take values between 0 and 1. The value is defined as the fraction of EEG not spent in suppression. The closer the value of the BCI is to 1, the more continuous the EEG is. Suppressions were defined as segments with amplitudes < 10 µV for at least 500 ms. A BCI of 0 indicates a completely suppressed EEG.

The BSAR was defined as the ratio between the amplitudes of suppressed EEG segments and non-suppressed EEG segments within an epoch. The BSAR was only calculated if  $0.01 \leq BCI \leq 0.99$ , otherwise BSAR = 1. In case of  $BSAR \geq 4$ , the epoch was visually checked on any remaining artefacts and excluded when necessary.

Both BCI and BSAR were calculated per artefact-free channel, after which the average over all channels was used for further analysis.

The BCI/BSAR prediction model was then defined as:

$$P_{good} = \frac{BCI}{1 + \exp(k \cdot (BSAR - BSAR_0))}$$

where  $P_{good}$  represents the chance of a good outcome. The coefficient  $BSAR_0$  represents the value for which the maximally achievable  $P_{good}$  is 0.5, and  $k$  determines how rapidly  $P_{good}$  approaches zero for  $BSAR$  values above  $BSAR_0$ . Because the coefficients are strongly time-dependent, separate models for 12, 24, 48 and 72 hours after cardiac arrest have been created by Ruijter et al.[13].

BCI,  $BSAR$  and  $P_{good}$  were calculated at 12, 24, 48 and 72 hours after cardiac arrest for every patient, if an artefact-free epoch was available at that time point. Thresholds for prediction of good and poor outcome described by Ruijter et al. were used. Patients' EEG's were classified as good, poor or intermediate based on these thresholds at 12, 24, 48 and 72 hours after cardiac arrest.

#### *Visual MRI analysis*

The DWI, FLAIR and SWI scans were visually scored by two independent neuroradiologists who were blinded to the patient's clinical status, medication and neurological outcome.

Cytotoxic oedema as a result of postanoxic encephalopathy causes restriction of water diffusion in the brain. On DWI scans, areas with diffusion restriction appear hyperintense. We therefore use DWI scans to visualize the extent of cytotoxic oedema.

Vasogenic oedema leads to an increase in water molecules close to the ventricles. Because CSF appears hypointense and water molecules in the brain appear hyperintense on FLAIR images, we use these scans to visualize the extent of vasogenic oedema in the brain.

DWI and FLAIR scans were graded using a semi-quantitative scoring system of predefined brain regions on a scale from 0 (no damage) to 4 (severely damaged) (table 2.2) [35]. Reviewers obtained a Fazekas score on FLAIR images and were instructed to only score damage directly related to the cardiac arrest. Consensus was sought when the scores of the two reviewers lay  $>1$  apart, otherwise, the average score of the reviewers was used.

The FLAIR score, DWI score, deep grey nuclei (DGN) score, and cortex score were calculated by adding up all scores of the corresponding brain regions as shown in table 2.2. Furthermore, we calculated an overall score by adding up all scores of the DWI and FLAIR scan.

TABLE 2.2 BRAIN REGIONS ASSESSED FOR VISUAL MRI ANALYSIS. COLOURS AND PATTERNS INDICATE BRAIN REGIONS CORRESPONDING TO DWI SCORE, FLAIR SCORE, CORTEX SCORE AND DGN SCORE.

	DWI	FLAIR
Frontal cortex	Cortex score	DGN score
Parietal cortex		
Temporal cortex		
Occipital cortex		
Insula		
Hippocampus		
Caudate nucleus	DGN score	DGN score
Putamen		
Globus pallidus		
Thalamus		
Frontal white matter	DWI score	FLAIR score
Parietal white matter		
Temporal white matter		
Occipital white matter		
Corpus callosum		
Midbrain		
Pons		
Medulla		
Cerebellar cortex		
Cerebellar white matter		
Dentate nucleus		

DWI score  
FLAIR score  
Cortex score  
DGN score

SWI images highlight deoxygenated blood. Patients with decreased oxygen extraction or decreased oxygen delivery to the brain show changes in the amount of deoxygenated blood in the brain. The veins of these patients therefore appear either more, or less prominent than normally.

SWI images were scored using a prominence of vein score. The deep medullary veins (DMVs) and cortical veins were scored between 1 and 7 (1=absent veins, 7=extremely prominent veins) [36]. In addition, the number of microbleeds was counted on these scans.

### Quantitative MRI analysis

Quantitative analysis based on the ADC maps was performed using MATLAB R2019a (The MathWorks Inc., Natick, Massachusetts, United States) and SPM12 (The FIL Methods Group, London, United Kingdom). ADC maps and anatomical T1 images were coregistered [37]. Thereafter, the T1 images were segmented based on tissue probability maps for grey matter, white matter, CSF, soft tissue and air/background for European brains provided by SPM12. Regional anatomic masks of grey matter, white matter and whole brain were created based on the 75% probability maps (figure 2.1). All voxels with ADC values below  $200 \times 10^{-6} \text{ mm}^2/\text{s}$  or above  $2000 \times 10^{-6} \text{ mm}^2/\text{s}$  were removed to exclude artefacts and CSF [16, 25]. Mean ADC values of the whole brain tissue, proportions of brain tissue with an ADC below  $650 \times 10^{-6} \text{ mm}^2/\text{s}$  and below  $450 \times 10^{-6} \text{ mm}^2/\text{s}$  [16], mean ADC values of the grey matter, mean ADC values of the white matter, and the ratio between mean ADC values of grey and white matter were calculated.

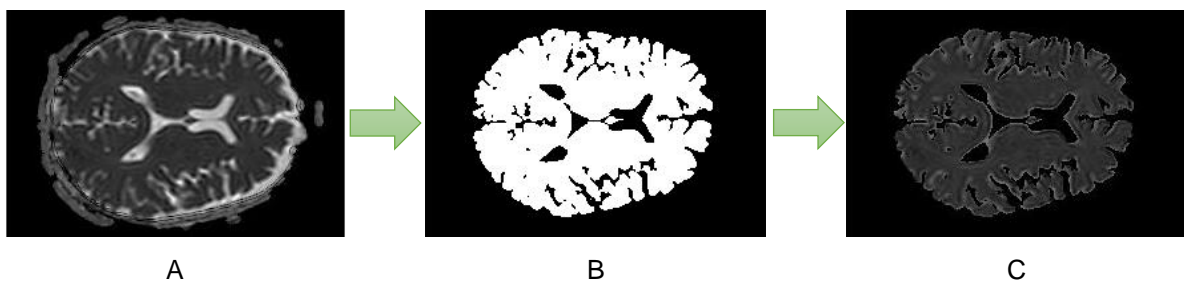


FIGURE 2.1 A REPRESENTS THE ADC MAP OF A PATIENT. THE MAP SHOWS CSF, SKIN AND ARTEFACTS THAT SHOULD BE REMOVED. PANEL B REPRESENTS THE WHOLE BRAIN MASK THAT WAS MADE BASED ON THE T1 IMAGE OF THIS PATIENT. PANEL C REPRESENTS THE RESULTING ADC MAP THAT ONLY CONTAINS THE GREY AND WHITE MATTER OF THE BRAIN. THIS MAP IS USED FOR FURTHER ANALYSIS.

#### 2.1.7 Statistical analysis

Data are presented as median (interquartile range (IQR)). To compare patients with good and poor neurological outcome on a group level, we used chi-squared tests for ordinal variables and Mann Whitney-U tests for continuous variables. Correlations between quantitative MRI and EEG measures were assessed using Pearson's correlation coefficients.

For each MRI parameter we plotted a receiver operating characteristics (ROC) curve and determined the sensitivity (95%CI) for good neurological outcome at 90% specificity and for poor neurological outcome at 100% specificity.

We chose the visual and quantitative MRI parameters with highest sensitivity for predicting good or poor neurological outcome as the most promising parameters. These were used to assess the additional value of the MRI, in addition to the EEG, for prediction of good or poor neurological outcome after cardiac arrest. Additional value is expressed as increase in sensitivity to predict poor or good outcome at specificity levels of 100% and 90%, respectively. Good or poor outcome is predicted when at least one of the parameters exceeds the threshold for the prediction of either good or poor outcome.

P-values < 0.05 were assumed statistically significant. All statistical analyses were performed using IBM SPSS Statistics 25, R version 3.5.3 and Matlab R2019a.

## 2.2 RESULTS

We included 30 comatose patients after cardiac arrest between June 2018 and October 2019, 23 in Rijnstate and 7 in Radboudumc. Complete follow-up was achieved in 25 patients and in the remaining 5 patients CPC score at 3 months follow-up was used. Poor neurological outcome occurred in 14 patients (47%), of whom 10 died. Table 2.3 shows patient characteristics of patients with good and poor neurological outcome and differences between the two groups. Patients with a poor neurological outcome had a longer time to ROSC than patients with a good neurological outcome ( $p=0.003$ ). Furthermore, EEG recordings were stopped later in patients with poor neurological outcome ( $p<0.001$ ). Figure 2.2 shows typical examples of the EEG at 12 hours after cardiac arrest and the ADC map and DWI image at 2-4 days after cardiac arrest of a patient with good (A) and poor (B) neurological outcome.

TABLE 2.3 PATIENT CHARACTERISTICS AND DIFFERENCES BETWEEN PATIENTS WITH GOOD AND POOR NEUROLOGICAL OUTCOME. CONTINUOUS DATA ARE SHOWN AS MEDIAN (IQR).

	All patients	CPC 1-2	CPC 3-5	p-value
<b>Patients, n (%)</b>	30 (100%)	16 (53%)	14 (47%)	
<b>Female, n (%)</b>	8 (27%)	4 (25%)	4 (29%)	0.825
<b>Age</b>	62.0 (52.0-70.8)	58.5 (52.0-64.0)	66.5 (53.0-74.8)	0.240
<b>Initial rhythm, n (%)</b>				0.209
- <b>Shockable</b>	28 (93%)	16 (100%)	12 (86%)	
- <b>Non-shockable</b>	2 (7%)	0 (0%)	2 (14%)	
<b>Time to ROSC (min)</b>	17.0 (10.0-21.3)	15.0 (10.0-17.5)	22.5 (17.5-37.5)	0.003 **
<b>Time MRI day 3 (h)</b>	75.3 (52.0-98.1)	74.1 (46.5-99.5)	75.3 (65.4-96.8)	0.667
<b>Start time EEG (h)</b>	9.7 (5.5-15.2)	9.7 (4.8-13.5)	8.8 (5.5-16.1)	0.683
<b>Stop time EEG (h)</b>	58.6 (37.5-59.0)	37.9 (31.7-59.0)	74.0 (53.8-99.0)	< 0.001 **

Asterisks indicate significant differences between groups (\*\* indicates  $p < 0.01$ ).

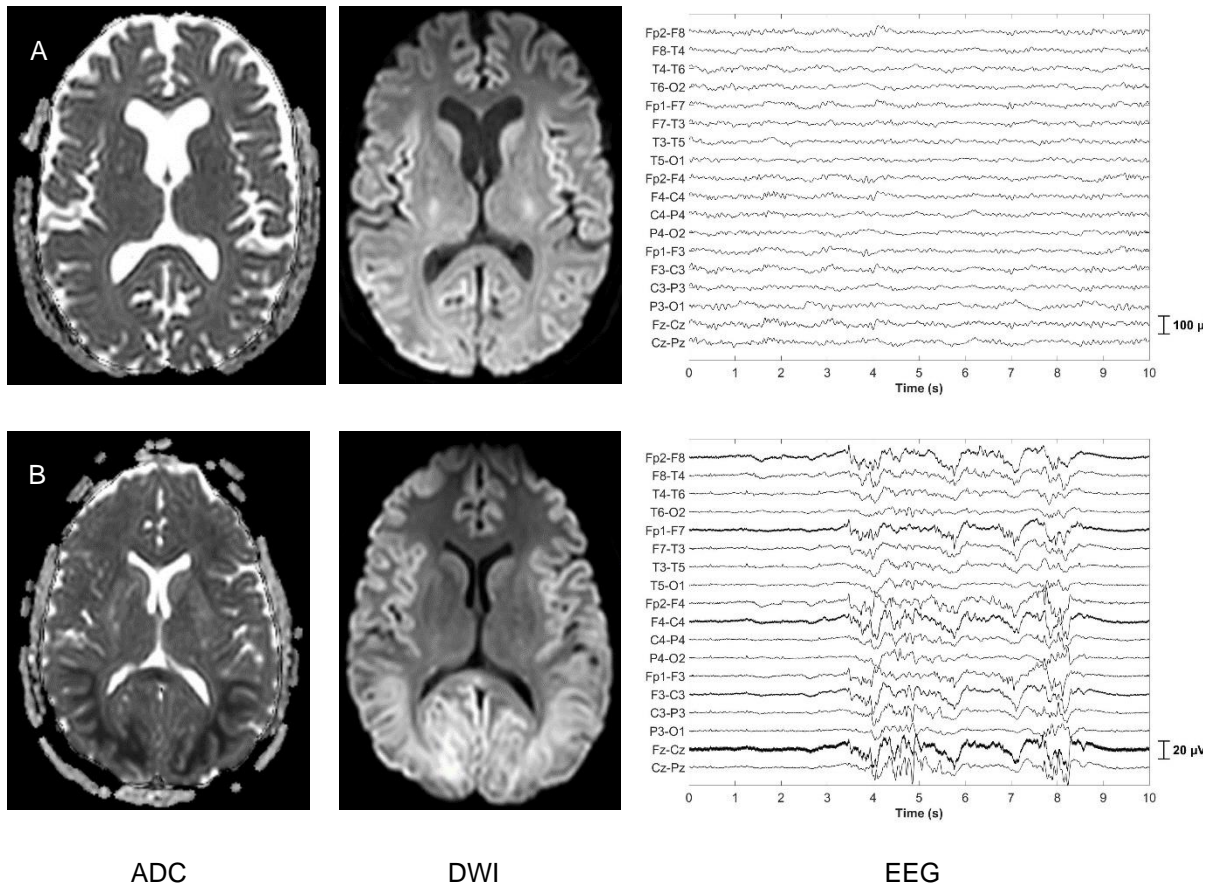


FIGURE 2.2 A REPRESENTS THE ADC MAP, DWI IMAGE AND EEG OF A PATIENT WITH GOOD NEUROLOGICAL RECOVERY. THE ADC MAP AND DWI IMAGE DO NOT SHOW ANY HYPOTENSE OR HYPERINTENSE REGIONS, RESPECTIVELY. THE EEG SHOWS A CONTINUOUS PATTERN. PANEL B REPRESENTS THE ADC MAP, DWI IMAGE AND EEG OF A PATIENT WITH POOR NEUROLOGICAL RECOVERY. THE ADC MAP SHOWS HYPOTENSE REGIONS IN THE OCCIPITAL LOBE, WHILE THE DWI IMAGE SHOWS HYPERINTENSE REGIONS IN THE OCCIPITAL LOBE, INDICATING DIFFUSION RESTRICTION.

### 2.2.1 Visual EEG classification

At 6 or 12 hours after cardiac arrest, 38% of the patients with good neurological recovery showed a favourable EEG pattern, compared to 14% of the patients with poor neurological outcome. An unfavourable pattern at 6, 12 or 24 hours after cardiac arrest was seen in 21% of the patients with poor neurological outcome, and never in patients with good outcome (figure 2.3). Results of visual EEG classification per time point are shown in appendix B.

Based on the combined visual EEG classification poor neurological outcome can be predicted with a sensitivity of 21% (95%CI: 5-51%) at a specificity of 100% (95%CI: 79-100%). Good neurological outcome can be predicted with a sensitivity of 38% (95%CI: 15-65%) at a specificity of 78% (95%CI: 40-97%).

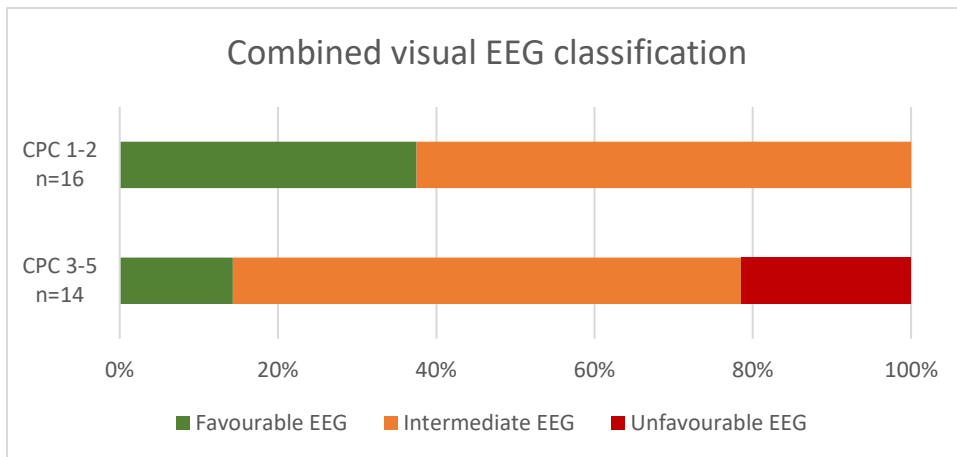


FIGURE 2.3 PERCENTAGES OF PATIENTS WITH FAVOURABLE, INTERMEDIATE AND UNFAVOURABLE EEGS BASED ON VISUAL EEG CLASSIFICATION IN GROUPS WITH GOOD AND POOR NEUROLOGICAL OUTCOME.

### 2.2.2 Quantitative EEG analysis

At 12 and 24 hours after cardiac arrest 83% and 92% of all patients with a good neurological outcome had a favourable quantitative EEG, respectively. None of the EEGs of these patients was classified as unfavourable and at 48 and 72 hours all EEGs were intermediate (figure 2.4).

Of all patients with poor neurological outcome 25% and 50% had a favourable EEG at 12 and 24 hours after cardiac arrest, respectively. 38% of the EEGs at 12 hours and 25% of the EEGs at 24 hours after cardiac arrest were unfavourable in this group. Highest sensitivity for prediction of poor neurological outcome is reached at 12 hours after cardiac arrest.

At 12 hours after cardiac arrest, poor neurological outcome can be predicted with a sensitivity of 38% (95%CI: 9-76%) at 100% specificity (95%CI: 75-100%) when only taking all available EEGs into account. Good neurological outcome can be predicted with 75% sensitivity (95%CI: 43-95%) at 75% specificity (95%CI: 35-97%) when only taking all available EEGs into account.

When we take the patients who do not have an EEG available at 12 hours after cardiac arrest into account, sensitivity for prediction of poor neurological outcome reaches 21% (95%CI: 5-51%) at 100% specificity (95%CI: 79-100%). Good neurological outcome can then be predicted with a sensitivity of 56% (95%CI: 30-80%) at 86% specificity (95%CI: 57-98%).

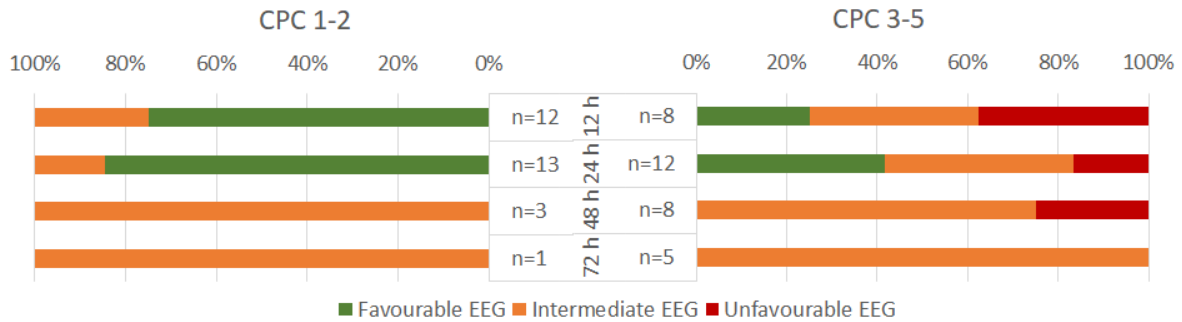


FIGURE 2.4 PERCENTAGES OF PATIENTS WITH FAVOURABLE, INTERMEDIATE AND UNFAVOURABLE EEGS BASED ON QUANTITATIVE EEG ANALYSIS AT 12, 24, 48 AND 72 HOURS AFTER CARDIAC ARREST IN GROUPS WITH GOOD AND POOR NEUROLOGICAL OUTCOME FOR ALL PATIENTS WITH AN EEG AVAILABLE AT SPECIFIC TIMEPOINTS.

### 2.2.3 Visual MRI analysis

Most abnormalities were found in the cortex and temporal white matter in patients with poor neurological outcome on both DWI images. None of the patients with good neurological outcome showed abnormalities in the caudate nucleus, putamen, globus pallidus and thalamus, while 6, 5, 5 and 1 patients with poor neurological recovery had abnormalities in those regions on the DWI, respectively. On the FLAIR images 4 patients with poor neurological outcome showed abnormalities in the caudate nucleus, 3 patients in the putamen and thalamus, and 1 patient in the globus pallidus. 6 patients with poor neurological outcome had abnormalities in the hippocampus on the DWI, while none of the patients with good neurological outcome did (table 2.4).

Significant differences between patients with good and poor neurological outcome were found for the Cortex score and DGN score ( $p=0.002$  and  $p<0.001$ , respectively) (figure 2.5). At the right ROC curves are shown for prediction of poor neurological outcome. Group differences of the other visual MRI scores can be found in appendix C.

Highest sensitivity for predicting poor neurological outcome reached by using only one score was by using the DGN score (sensitivity 71% (95%CI: 42-92%) at 100% specificity (95%CI: 74-100%)). Good neurological outcome can be predicted with a sensitivity of 42-43% with Cortex score or DWI score. We chose the cortex score as the most promising parameter for prediction of good neurological outcome, because it requires the fewest brain regions to be scored. Combined prediction was based on at least one of the scores exceeding the threshold for prediction of good or poor outcome. When combining all visual MRI scores good neurological outcome can be predicted with a sensitivity of 75% (95%CI: 48-93%) and poor neurological outcome with a sensitivity of 86% (95%CI: 57-98%) (table 2.5).

TABLE 2.4 RESULTS OF VISUAL ANALYSIS OF DWI AND FLAIR SCANS. NUMBERS REPRESENT THE PERCENTAGE OF PATIENTS WITH GOOD AND POOR NEUROLOGICAL OUTCOME WITH ABNORMALITIES IN SPECIFIC BRAIN REGIONS ON DWI AND FLAIR IMAGES, COLOURS REPRESENT THE PERCENTAGE OF PATIENTS WITH ABNORMALITIES IN SPECIFIC BRAIN REGIONS (RED = 100%, GREEN = 0%).

	DWI		FLAIR	
	CPC 1-2	CPC 3-5	CPC 1-2	CPC 3-5
Frontal cortex	14%	71%	0%	36%
Parietal cortex	7%	71%	7%	36%
Temporal cortex	0%	64%	0%	21%
Occipital cortex	7%	79%	0%	36%
Insula	7%	43%	0%	21%
Hippocampus	0%	43%	6%	29%
Caudate nucleus	0%	36%	0%	29%
Putamen	0%	36%	0%	21%
Globus pallidus	0%	7%	0%	7%
Thalamus	0%	14%	0%	21%
Frontal white matter	14%	7%	14%	0%
Parietal white matter	7%	14%	7%	0%
Temporal white matter	0%	64%	0%	21%
Occipital white matter	0%	7%	0%	0%
Corpus callosum	0%	7%	0%	0%
Midbrain	7%	0%	7%	0%
Pons	0%	0%	0%	0%
Medulla	0%	0%	0%	0%
Cerebellar cortex	14%	36%	7%	28%
Cerebellar white matter	7%	7%	14%	0%
Dentate nucleus	0%	0%	0%	0%

TABLE 2.5 PREDICTIVE VALUES OF SCORES BASED ON VISUAL ANALYSIS OF DWI AND FLAIR IMAGES FOR PREDICTING GOOD AND POOR NEUROLOGICAL OUTCOME.

	Predicting good outcome			Predicting poor outcome		
	Threshold	Sensitivity (95%CI)	Specificity (95%CI)	Threshold	Sensitivity (95%CI)	Specificity (95%CI)
<b>DGN score</b>	N.A.	N.A.	N.A.	≥ 1	71% (42-92)	100% (74-100)
<b>Cortex score</b>	≤ 2	42% (15-72)	93% (66-100)	≥ 20.5	57% (29-82)	100% (74-100)
<b>DWI score</b>	≤ 1	43% (18-71)	100% (77-100)	≥ 17	64% (35-87)	100% (77-100)
<b>FLAIR score</b>	= 0	21% (5-51)	93% (66-100)	≥ 11.5	36% (13-65)	100% (77-100)
<b>Overall score</b>	≤ 6	58% (28-85)	93% (66-100)	≥ 30	57% (29-82)	100% (74-100)
<b>Combined</b>	At least one score > threshold	75% (48-93)	93% (66-100)	At least one score > threshold	86% (57-98)	100% (79-100)

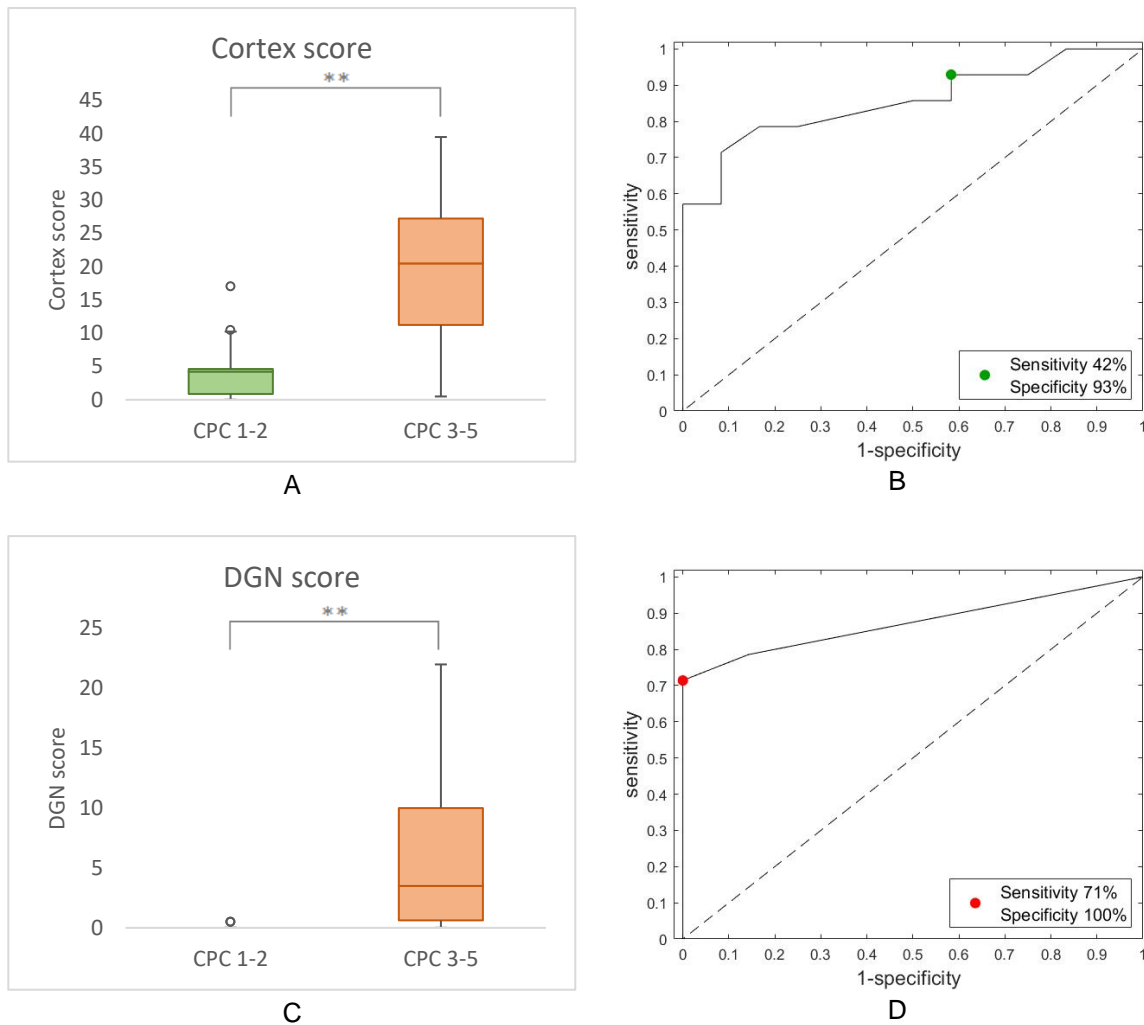


FIGURE 2.5 A AND B REPRESENT GROUP DIFFERENCES AND PREDICTIVE VALUE FOR GOOD NEUROLOGICAL OUTCOME OF THE CORTEX SCORE. THE GREEN DOT REPRESENTS A SENSITIVITY OF 43% (100% SPECIFICITY) AT A THRESHOLD OF 1. C AND D REPRESENT GROUP DIFFERENCES AND PREDICTIVE VALUE FOR POOR NEUROLOGICAL OUTCOME OF THE DGN SCORE. THE RED DOT REPRESENTS A SENSITIVITY OF 71% (100% SPECIFICITY) AT A THRESHOLD OF 1. ASTERISKS INDICATE SIGNIFICANT DIFFERENCES BETWEEN GROUPS (\*\*  $P < 0.01$ ).

Visual SWI analysis showed no significant differences between patients with good and poor neurological outcome for both prominence of DMV and cortical veins ( $p = 0.425$  and  $p = 0.290$ , respectively). Patients with good neurological outcome had a prominence of vein score of 2.5 (1.8-2.8) and 4.0 (3.0-4.5) for the DMVs and cortical veins, respectively. Patients with poor neurological outcome had a prominence of vein score of 2.0 (2.0-2.5) and 4.0 (3.5-4.5) for the DMVs and cortical veins, respectively.

### 2.2.4 Quantitative MRI analysis

Whole brain mean ADC, grey matter mean ADC and grey-to-white matter ratio were significantly smaller in patients with poor neurological outcome compared to patients with good neurological outcome ( $p=0.034$ ,  $p=0.019$ , and  $p=0.022$  respectively).

Patients with poor neurological outcome showed significant higher proportions of brain volume with an ADC value below  $450 \times 10^{-6} \text{ mm}^2/\text{s}$  ( $p=0.019$ , figure 2.6) than patients with good neurological recovery. Group differences of the other quantitative MRI measures are shown in Appendix E.

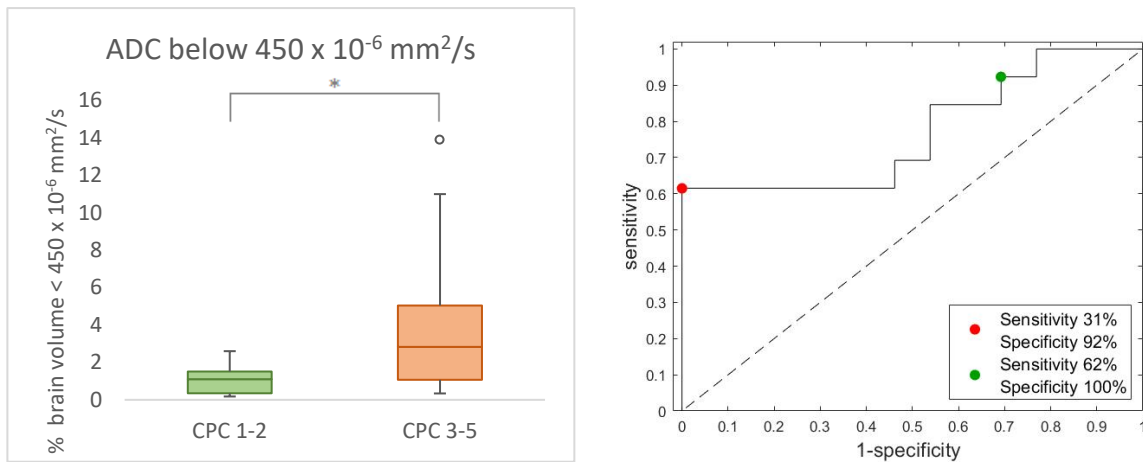


FIGURE 2.6 GROUP DIFFERENCES AND PREDICTIVE VALUE OF THE PROPORTION OF BRAIN VOLUME WITH AN ADC VALUE BELOW  $450 \times 10^{-6} \text{ mm}^2/\text{s}$  FOR GOOD AND POOR NEUROLOGICAL OUTCOME. THE GREEN DOT REPRESENTS A SENSITIVITY OF 31% (92% SPECIFICITY) AT A THRESHOLD OF 0.35%. THE RED DOT REPRESENTS A SENSITIVITY OF 62% (100% SPECIFICITY) AT A THRESHOLD OF 2.82%. ASTERISKS INDICATE SIGNIFICANT DIFFERENCES (\*  $P < 0.05$ ).

Highest individual sensitivity for prediction of poor neurological outcome is reached by using mean ADC value of the whole brain, mean ADC value of the grey matter or the proportion of brain volume with an ADC value below  $450 \times 10^{-6} \text{ mm}^2/\text{s}$  (sensitivity of 62% (95%CI: 32-86%) at 100% specificity (95%CI: 75-100%)) (table 2.6). Highest individual sensitivity for prediction of good neurological outcome is reached using the proportion of brain value with an ADC value below  $450 \times 10^{-6} \text{ mm}^2/\text{s}$  (sensitivity of 31% (95%CI: 9-61%) at 92% specificity (95%CI: 64-100%)). Combined prediction was based on at least one of the parameters exceeding the threshold for prediction of good or poor outcome. When combining all quantitative MRI parameters sensitivity reaches 64% (95%CI: 35-87%) at 100% specificity (95%CI: 79-100%) for prediction of poor neurological outcome. Good neurological outcome can be predicted with a sensitivity of 44% (95%CI: 20-70%) at 93% specificity (95%CI: 66-100%).

TABLE 2.6 SENSITIVITY AND SPECIFICITY OF THE SIX QUANTITATIVE MRI PARAMETERS WITH CORRESPONDING THRESHOLDS FOR PREDICTING POOR NEUROLOGICAL OUTCOME.

	Predicting good outcome			Predicting poor outcome		
	Threshold	Sensitivity (95%CI)	Specificity (95%CI)	Threshold	Sensitivity (95%CI)	Specificity (95%CI)
<b>Whole brain mean ADC</b>	$\geq 909.31 \times 10^{-6} \text{ mm}^2/\text{s}$	15% (2-45)	100% (75-100)	$\leq 822.29 \times 10^{-6} \text{ mm}^2/\text{s}$	62% (32-86)	100% (75-100)
<b>Grey matter mean ADC</b>	$\geq 942.64 \times 10^{-6} \text{ mm}^2/\text{s}$	23% (5-54)	100% (75-100)	$\leq 847.75 \times 10^{-6} \text{ mm}^2/\text{s}$	62% (32-86)	100% (75-100)
<b>White matter mean ADC</b>	$\geq 858.93 \times 10^{-6} \text{ mm}^2/\text{s}$	8% (0-36)	92% (64-100)	$\leq 705.51 \times 10^{-6} \text{ mm}^2/\text{s}$	23% (5-54)	100% (75-100)
<b>Grey-white-matter ratio</b>	$\geq 1.21$	23% (5-54)	92% (64-100)	$\leq 1.07$	31% (9-61)	100% (75-100)
<b>Proportion of brain volume with ADC &lt; 650 x 10<sup>-6</sup> mm<sup>2</sup>/s</b>	$\leq 3.79\%$	8% (0-36)	100% (75-100)	$\geq 21.43\%$	46% (19-75)	100% (75-100)
<b>Proportion of brain volume with ADC &lt; 450 x 10<sup>-6</sup> mm<sup>2</sup>/s</b>	$\leq 0.35\%$	31% (9-61)	92% (64-100)	$\geq 2.82\%$	62% (32-86)	100% (75-100)
<b>Combined</b>		44% (20-70)	93% (66-100)		64% (35-87)	100% (79-100)

### 2.2.5 Association between EEG and MRI measures

The BCI is negatively correlated with multiple quantitative MRI measures (appendix F). Highest correlations are found between the BCI at 12 hours and the cortex score ( $r=-0.821$ ,  $p<0.001$ ), BCI at 12 hours and the DWI score ( $r=-0.805$ ,  $p<0.001$ ), BCI at 12 hours and the Overall score ( $r=-0.760$ ,  $p=0.001$ ) and BCI at 48 hours and grey-white matter ratio on the ADC map ( $r=0.751$ ,  $p=0.008$ ).

Patients with unfavourable EEG patterns showed higher Cortex scores, DWI scores and Overall scores than patients with favourable and intermediate EEG patterns (table 2.7). However, none of these differences are statistically significant.

TABLE 2.7 VISUAL MRI SCORES GROUPED BY DIFFERENT EEG CATEGORIES. DATA ARE PRESENTED AS MEDIAN (IQR).

	DGN score	Cortex score	DWI score	FLAIR score	Overall score
Favourable EEG (n=8)	0.0 (0.0-0.5)	4.5 (2.0-10.5)	5.5 (0.3-11.8)	3.0 (1.0-7.0)	8.5 (4.8-19.5)
Intermediate EEG (n=18)	0.8 (0.0-7.0)	9.0 (1.8-26.0)	10.5 (2.0-24.5)	5.0 (1.4-13.1)	15.5 (5.5-37.3)
Unfavourable EEG (n=3)	0.5 (0.1-8.0)	20.5 (13.0-20.5)	31.5 (15.4-34.1)	4.5 (2.3-6.0)	38.0 (18.1-39.1)

### 2.2.6 Additional predictive value of MRI measures in addition to the EEG

To estimate the additional value of MRI on EEG, the measures with the highest predictive values of all categories were considered. For prediction of poor neurological outcome we compared combined visual EEG classification,  $P_{good}$  at 12 hours after cardiac arrest, DGN score and the proportion of brain volume with ADC value below  $450 \times 10^{-6} \text{ mm}^2/\text{s}$ . Patients with at least one of these parameters exceeding the threshold for poor outcome were predicted to have poor neurological outcome. For prediction of good neurological outcome, we compared combined visual EEG classification,  $P_{good}$  at 12 hours after cardiac arrest, Cortex score and the proportion of brain volume with ADC value below  $450 \times 10^{-6} \text{ mm}^2/\text{s}$ . Patients with at least one of these parameters exceeding the threshold for good outcome were predicted to have good neurological recovery. When patients had different measures exceeding thresholds for both good and poor outcome, patient's outcome was predicted as poor.

The combined visual EEG classification and  $P_{good}$  together predict good neurological outcome with a sensitivity of 62% (95%CI: 35-85%) at a specificity of 81% (95%CI: 54-96%) and poor neurological outcome with a sensitivity of 21% (95%CI: 5-51%) at a sensitivity of 100% (95%CI: 79-100%). The most promising MRI parameters together could predict good neurological outcome with a sensitivity of 31% (95%CI: 11-59%) at a specificity of 100% (95%CI: 77-100%) and poor neurological outcome with a sensitivity of 79% (95%CI: 49-95%) at a specificity of 100% (95%CI: 79-100%). Adding the chosen MRI parameters to the chosen EEG parameters increased the sensitivity for prediction of good neurological outcome to 75% (95%CI: 48-93%) at 86% specificity (95%CI: 57-98%). Poor outcome can then be predicted with a sensitivity of 86% (95%CI: 57-98%) at 100% specificity (95%CI: 79-100%) (table 2.8).

TABLE 2.8 SENSITIVITY AND SPECIFICITY WITH CORRESPONDING 95% CONFIDENCE INTERVALS OF EEG AND MRI PARAMETERS AND THE COMBINATION FOR PREDICTING GOOD AND POOR NEUROLOGICAL OUTCOME AFTER CARDIAC ARREST.

	Predicting good outcome		Predicting poor outcome	
	Sensitivity	Specificity	Sensitivity	Specificity
<b>Visual EEG</b>	38% (15-65)	78% (40-97)	21% (5-51)	100% (79-100)
<b>Quantitative EEG</b>	56% (30-80)	86% (57-98)	21% (5-51)	100% (79-100)
<b>Visual MRI</b>	31% (11-59)	100% (77-100)	71% (42-92)	100% (79-100)
<b>Quantitative MRI</b>	44% (20-70)	93% (66-100)	64% (35-87)	100% (79-100)
<b>Combined</b>	75% (48-93)	86% (57-98)	86% (57-98)	100% (79-100)

## 2.3 DISCUSSION

With this prospective cohort study, including 30 patients from 2 hospitals, we show that visual and quantitative analyses of structural MRI scans on day 2-4 after cardiac arrest hold potential to improve neurological outcome prediction after cardiac arrest, when added to continuous EEG recording.

Abnormalities in the deep grey nuclei on both FLAIR and DWI images were invariably associated with poor neurological outcome. Furthermore, a proportion of brain with ADC value below  $450 \times 10^{-6} \text{ mm}^2/\text{s}$  of at least 2.82% could identify 64% of the patients with poor neurological outcome with a specificity of 100%. Visual and quantitative EEG measures could identify 21% of all patients with poor neurological outcome. The addition of visual and quantitative MRI measures increased this to 86% in our population.

These results suggest that performing an MRI scan on day 2-4 after cardiac arrest could be of great additional value on performing continuous EEG recordings for outcome prediction after cardiac arrest. This would help patients' families and clinicians in making informed decisions on continuation or withdrawal of treatment.

### *Visual EEG classification*

Visual EEG classification could identify only 21% (95%CI: 5-51%) of all patients with a poor neurological outcome, while previous research showed a sensitivity of 52% (95%CI: 47-58%) [14]. This could be explained by the difference in patient inclusion in both studies. We included only adult comatose patients that underwent an MRI scan on day 2-4 after cardiac arrest. Patients who died before an MRI scan could be performed were therefore not included in our study. However, these patients were likely to have unfavourable EEG patterns. We acted reserved regarding treatment withdrawal. The EEG did not influence decisions on withdrawal of treatment. Only patients with absent N20 responses on the SSEP or patients with non-neurological reasons of death were withdrawn from treatment before MRI could take place.

*Quantitative EEG analysis*

Most promising quantitative EEG parameter was  $P_{good}$  at 12 hours after cardiac arrest. Quantitative EEG parameters were particularly predictive for neurological outcome at 12 hours after cardiac arrest, because we saw that the EEG of many patients with poor neurological outcome normalizes after these 12 hours. Therefore, the prediction of good neurological outcome becomes less specific after more than 12 hours after cardiac arrest. Furthermore, less patients show unfavourable EEG patterns after this period, which decreases the sensitivity for prediction of poor outcome.

Based on  $P_{good}$  at 12 hours after cardiac arrest, we could predict poor neurological outcome with a sensitivity of 21% and good neurological outcome with a sensitivity of 56%. Previous research showed that poor neurological outcome could be predicted with a sensitivity of 50% and good neurological outcome with a sensitivity of 52% at 12 hours after cardiac arrest [13]. Differences in patient inclusion could again explain this lower sensitivity for the prediction of poor neurological outcome in our study.

*Visual MRI analysis*

Visual analysis of DWI and FLAIR images showed most abnormalities in the cortex, DGN and temporal white matter for patients with poor neurological outcome. Patients with a poor outcome had significant higher Cortex scores, DGN scores, DWI scores, FLAIR scores and overall scores compared to patients with good neurological outcome. Most promising scores for prediction of poor and good neurological outcome were DGN score and cortex score, respectively. Abnormalities in the cortex and DGN are in accordance with previous literature [20, 21, 35, 38, 39]. Both the cortex and DGN are susceptible to damage caused by hypoxia [7, 8, 40, 41]. The cortex and thalamus play a major role in arousal, awareness and consciousness [42, 43]. Extensive damage to the cortex will therefore result in unconsciousness and a poor neurological outcome. The basal ganglia (caudate nucleus, putamen and globus pallidus) are important for movement and coordination [42, 43]. Patients with damage to the basal ganglia will therefore encounter movement disorders and dyscoordination, resulting in lower CPC scores. This explains why DGN and cortex score are predictive for neurological outcome after cardiac arrest.

Visual SWI analysis showed no significant differences in the prominence of deep medullary veins and cortical veins between patients with good and poor neurological outcome. Previous research on neurological outcome prediction in neonatal patients with hypoxic-ischemic injury showed that patients with abnormal prominence of DMVs were likely to have worse neurological outcome than patients with normal prominence of DMVs. In this case, a low prominence of veins supposedly indicates an increase in oxygen bound haemoglobin in the DMVs, due to less uptake by damaged brain tissue. An increased prominence might indicate a decrease in oxygen bound haemoglobin, since blood flow is restricted to non-active brain tissue. This measure is not yet validated in adult patients and physiological and metabolic influences on the prominence of vein score are largely unknown. At this moment, the prominence of vein score is likely not to contribute to outcome prediction in this patient group. The difference in finding could be explained by the difference in patient characteristics.

*Quantitative MRI analysis*

We found significant differences between patients with good and poor neurological outcome for whole brain mean ADC, grey matter ADC, grey to white matter ratio and proportion of brain with ADC below  $450 \times 10^{-6} \text{ mm}^2/\text{s}$ . No significant differences were found for white matter ADC. These results reflect the increased vulnerability of grey matter compared to white matter to cerebral anoxia. Highest sensitivity for prediction of poor neurological outcome at 100% specificity was reached using grey matter ADC and proportion below  $450 \times 10^{-6} \text{ mm}^2/\text{s}$ . Proportion of brain below  $450 \times 10^{-6} \text{ mm}^2/\text{s}$  could predict good neurological outcome with highest sensitivity and was therefore chosen as most promising quantitative MRI variable for predicting both good and poor neurological outcome.

Quantitative MRI analysis is an objective approach that is not sensitive to interrater differences. However, offline processing of the data is necessary, which makes it impossible to perform real time prediction based on quantitative MRI measures. Radiologists and neurologists are not yet used to this approach. This could complicate the introduction of this method in the clinical field.

*Association between EEG and MRI*

Strongest correlations between EEG and MRI parameters exist for BCI at 12 hours after cardiac arrest with the cortex score, DWI score and Overall score. This is in line with our expectations, since many patients with poor neurological outcome have both unfavourable EEGs and abnormalities on brain MRI. As described before, after 12 hours, pseudo-normalization of the EEG occurs in a large part of the patients with poor neurological outcome. This normalization induces a decrease in correlation between EEG and MRI parameters. We expected high correlations between the EEG and MRI during the phase in which many EEG abnormalities are present.

Patients with an unfavourable EEG based on visual EEG classification show higher cortex scores, DWI scores and overall scores. None of the differences was statistically significant, probably because of the small group sizes (only 3 patients with an unfavourable EEG).

The EEG reflects cortical electrical activity. High cortex scores imply extensive cortical damage and are therefore likely to correlate with unfavourable EEG patterns. Extensive overall brain damage and oedema displayed by the overall score, DWI score, and FLAIR score are likely to influence the cortical activity as well. However, not all patients with a disturbed EEG will also have abnormalities in the underlying structures of the brain. These patients do not show any structural changes on the MRI. However, it is likely that these patients suffer from functional damage of the brain that is not visible on the structural images we analysed in this thesis.

*Additional value of MRI on top of the EEG*

The addition of both visual and quantitative MRI measures to outcome prediction based on visual and quantitative EEG analysis increases sensitivity for the prediction of poor neurological outcome at 100% specificity. However, both visual and quantitative MRI analyses seem unsuitable for prediction of good neurological outcome after cardiac arrest. We expected the MRI to have additional value on the EEG for prediction of poor neurological outcome, because the EEG only represents the cortical electrical activity of the brain. The MRI can evaluate underlying structures as well and patients who do not show

severe abnormalities in cortical activity can still show abnormalities in underlying structures of the brain. These patients are likely to have an intermediate EEG, but an unfavourable MRI.

Based on EEG parameters, we could identify 3 of 14 patients with poor neurological outcome. MRI parameters could identify 8 more patients with poor neurological outcome that did not show any EEG abnormalities. Of all 16 patients with good neurological outcome, 10 could be identified based on EEG findings. Adding MRI parameters to this prediction only increased the number of patients correctly classified as good outcome to 11.

Thresholds for prediction of good or poor neurological outcome with EEG measures were based on previous research including 559-850 patients [13, 14]. Sensitivity and specificity for the prediction of good or poor neurological outcome therefore have small confidence intervals and the data is robust. We performed our MRI analysis on data of only 30 patients, resulting in wide confidence intervals and a high uncertainty about our data. Therefore, we probably overestimate the value of our MRI measures in addition to EEG measures.

Although we probably overestimate the value of our MRI measures, previous research also showed that a combination of both EEG and MRI measures improves poor outcome prediction compared to predicting based on either EEG or MRI [25-27].

#### *Limitations*

The primary limitation of this study is the small number of patients included. Because we based our MRI thresholds on only 30 patients, we are likely to overestimate the additional value of the MRI in addition to EEG.

Treating physicians were not completely blinded for EEG recordings and MRI scans. However, analyses were performed offline, blinded for patients' outcome. MRI scans and EEGs within 72 hours after cardiac arrest were not included in decisions on withdrawal of treatment. This decreases the bias of self-fulfilling prophecy.

Continuous EEG recordings were only started between 8 AM and 5 PM. Patients arriving just after 5 PM often lacked EEG measurements within 12 hours after cardiac arrest. This results in missing data and a lower sensitivity for prediction of both good and poor neurological outcome based on EEG parameters.

Neurological outcome may in some cases have been influenced by causes unrelated to the postanoxic encephalopathy. We did not exclude any patients that died from other causes than postanoxic encephalopathy or surviving patients whose daily living was strongly affected by other factors. Because none of the patients included has died from other causes than postanoxic encephalopathy, our results were not influenced by this. Post hoc analyses could be used to investigate the consequences on our findings of other factors than neurological changes influencing the CPC scores.

## 2.4 CONCLUSION

Visual and quantitative MRI analyses hold potential to increase sensitivity for prediction of good or poor neurological outcome after cardiac arrest, with equal reliability. Patients with poor neurological outcome have significantly higher proportions of brain volume with ADC value below  $450 \times 10^{-6} \text{ mm}^2/\text{s}$  and

significantly higher DGN and cortex scores than patients with good neurological outcome. To be able to generalize these findings and further assess the additional value of MRI parameters on top of continuous EEG recording, more patients are needed.



## CHAPTER 3

### NEUROLOGICAL OUTCOME PREDICTION BASED ON ULTRASOUND

The sheath surrounding the optic nerve is in continuation with the subarachnoid space. Therefore, rises in intracranial pressure (ICP) are transmitted to the optic nerve, resulting in swelling of the optic nerve sheath. This swelling can be measured using ocular ultrasound. We therefore expect patients with increased ICP as a result of cerebral oedema after cardiac arrest to have a large optic nerve sheath diameter (ONSD).

#### RESEARCH QUESTIONS

What is the predictive value of repeated ONSD measurements on the first three days after resuscitation, for good and poor neurological outcome of comatose patients after cardiac arrest?

- How does the ONSD change over time for patients with good and poor neurological outcome?
- What is the intrarater reliability of ultrasonographic ONSD measurements?

#### 3.1 METHODS

##### 3.1.1 Study Design

This is a prospective cohort study investigating the value of the ONSD for prediction of neurological outcome of comatose patients after cardiac arrest, admitted to the intensive care unit (ICU) of Rijnstate hospital. The Committee on Research Involving Human Subjects decided that the Medical Research Involving Human Subjects act did not apply for this study. Data for the current analyses were collected from December 2019 to February 2020.

##### 3.1.2 Study population

Consecutive adult comatose patients admitted to the ICU of Rijnstate Hospital were included. The Committee on Research Involving Human Subjects region Arnhem-Nijmegen waved the need for informed consent prior to study inclusion. Patients who regained consciousness were asked for verbal deferred consent. Exclusion criteria were pregnancy, traumatic head injury, eye surgery in medical history, pre-existing dependency in daily living (cerebral performance category (CPC) 3 or 4) or any relevant progressive brain illness. Measurements were only performed on comatose or adequately sedated patients.

##### 3.1.3 Standard of care

Patients were monitored and treated according to guidelines for comatose cardiac arrest patients as described in local ICU protocols. Targeted temperature management at 36 °C was induced as soon as possible after arrival at the emergency room or ICU and maintained for 24 hours. After 24 hours, passive rewarming was controlled to a speed of 0.25 °C or 0.5 °C per hour. In case of a temperature > 38 °C and a Glasgow Coma Scale (GCS) score ≤ 8, targeted temperature management was restarted at 36.5 °C to 37.5 °C for another 48 hours. Patients received a combination of propofol, midazolam and morphine for sedation.

### 3.1.4 Decisions on withdrawal of treatment

Withdrawal of treatment was considered at  $\geq 72$  hours after cardiac arrest, during normothermia, and off sedation. Decisions on withdrawal of treatment were based on national guidelines including incomplete return of brainstem reflexes, treatment-resistant myoclonus and bilateral absence of somatosensory evoked potentials (SSEPs) [9]. The ONSD was not included in decisions of treatment withdrawal and patients' therapists were blinded to ONSD measurements.

### 3.1.5 Data collection

#### *ONSD*

ONSD measurements were performed by trained personnel on day 1, 2 and 3 after resuscitation. The ONSD was measured using a linear ultrasound probe with a frequency range of 3-12 MHz using the Philips Affinity®. Sterile ultrasound gel was placed on the probe and a sterile ultrasound probe cover is placed over it, preventing ultrasound gel from touching the eye. The probe was placed transversally on the superior and lateral part of the upper eyelid, angled caudally and medially with the head 30° elevated. As little pressure as possible was put on the eye. The probe was adjusted to display the entrance of the optic nerve into the ocular globe [44]. The ONSD was measured 3 mm behind the retina. Three consecutive measurements per eye were performed each day.

#### *Neurological outcome*

The primary outcome measure was neurological outcome, defined by the score on the GCS at hospital discharge. GCS  $\geq 13$  indicated favourable neurological outcome, and GCS  $< 13$  indicated unfavourable neurological outcome.

### 3.1.6 Data analysis

Data analyses were performed offline using Matlab R2019a. We used average ONSD measurement and standard deviation per eye per day for further analysis.

Data were presented as median (IQR). To compare patients with good and poor neurological outcome on a group level, we used chi-squared tests for ordinal variables and Mann-Whitney U tests for continuous variables.

Sensitivity and specificity for prediction of good or poor neurological outcome were evaluated at different cut-off values for the ONSD, derived from the receiver operating characteristic (ROC)-analysis. We evaluated the sensitivity (95%CI) for the prediction of poor neurological outcome at 100% specificity and the sensitivity (95%CI) for the prediction of good neurological outcome at 90% specificity. The changes of ONSD over time were presented in a descriptive way.

Intraclass correlation coefficient and Cronbach's alpha were used for evaluation of repeatability of the measurements.

P-values  $< 0.05$  were assumed statistically significant. All statistical analyses were performed using IBM SPSS Statistics 25 and R version 3.5.3.

## 3.2 RESULTS

We included 11 consecutive comatose patients after cardiac arrest between December 2019 and February 2020. Poor neurological outcome occurred in 6 patients (55%), of whom 4 died. Table 3.1 shows patient characteristics of patients with good and poor neurological outcome and differences between the two groups. No significant differences between the groups were found for sex, age or time to ROSC.

TABLE 3.1 PATIENT CHARACTERISTICS AND DIFFERENCES BETWEEN PATIENTS WITH GOOD AND POOR NEUROLOGICAL OUTCOME. CONTINUOUS DATA ARE SHOWN AS MEDIAN (IQR).

	All patients	GCS $\geq$ 13	GCS < 13	p-value
<b>Patients, n (%)</b>	11 (100%)	5 (45%)	6 (55%)	
<b>Female, n (%)</b>	3 (27%)	2 (40%)	1 (17%)	0.387
<b>Age</b>	68.0 (51.0-76.0)	62.0 (43.0-72.5)	77.0 (55.5-81.3)	0.329
<b>Time to ROSC (min)</b>	23.0 (15.0-50.0)	20.0 (8.5-25.0)	40.0 (21.0-63.8)	0.052

### Missing data

At day 1 we measured 5 patients with good neurological recovery and 6 patients with poor neurological recovery. After day 1 we lost 1 patient due to waking up and 2 patients due to death. After day 2 we lost another 2 patients with poor neurological outcome due to death.

### Group differences

No significant differences in ONSD were present on day 1 and 2 between patients with good and poor neurological recovery. The ONSD measured on day 3 was significantly higher in patients with good neurological outcome, compared to patients with poor neurological outcome ( $p=0.016$ ) (figure 3.1).

Sensitivity for prediction of good neurological outcome was 20% (95%CI: 3-56%) at 100% specificity (95%CI: 74-100%) on day 1 (threshold ONSD  $\leq$  5.46 mm), and 13% (95%CI: 0-53%) at 100% specificity (95%CI: 63-100%) on day 2 (threshold ONSD  $\leq$  4.99 mm). Poor neurological outcome could be predicted with 8% sensitivity (95%CI: 0-38%) at 100% specificity (95%CI: 69-100%) at day 1 (threshold ONSD  $\geq$  7.07 mm), and with 13% sensitivity (95%CI: 0-53%) at 100% specificity (95%CI: 63-100%) at day 2 (threshold ONSD  $\geq$  7.13 mm). Prediction on day 3 was not performed because patients with poor neurological outcome had significant lower ONSD measurements than patients with good neurological outcome.

### Repeatability of the measurements

The intrarater reliability was 77.7% (95%CI: 67.3-85.7%) with  $p<0.001$  measured by the intra-class correlation coefficient. Cronbach's alpha was 0.915, which indicates an excellent internal consistency.

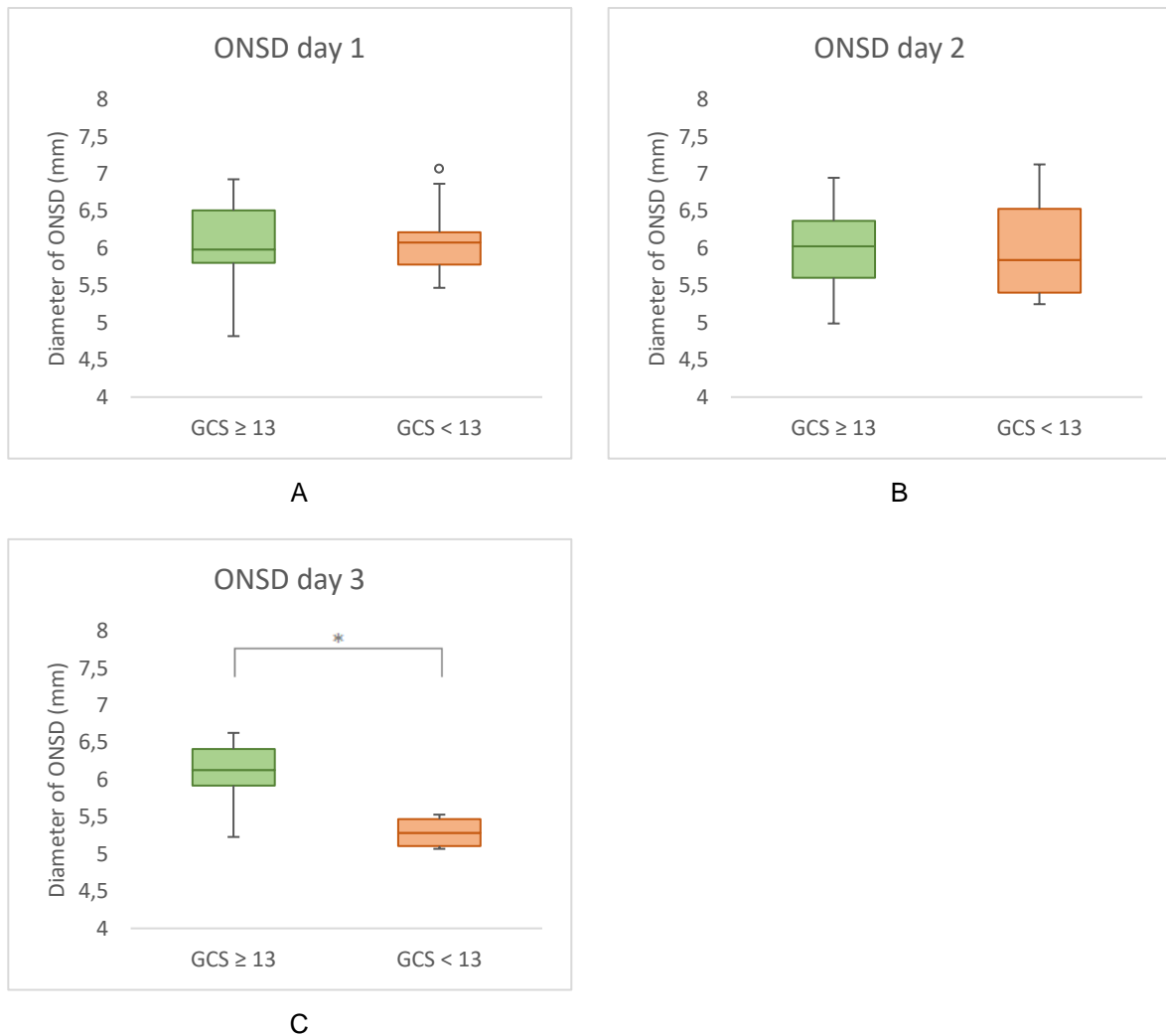


FIGURE 3.1 A REPRESENTS GROUP DIFFERENCES OF THE ONSD MEASURED ON DAY 1 AFTER CARDIAC ARREST. B REPRESENTS GROUP DIFFERENCES OF THE ONSD MEASURED ON DAY 2 AFTER CARDIAC ARREST. C REPRESENTS GROUP DIFFERENCES OF THE ONSD MEASURED ON DAY 3 AFTER CARDIAC ARREST. ASTERISKS INDICATE STATISTICALLY SIGNIFICANT DIFFERENCES (\* INDICATES  $P < 0.05$ ).

### Feasibility

Measurements of the ONSD were easy and cheap to perform. Measurements only took 10 minutes per day and did not obstruct daily care for these patients. Measurements can be performed by intensivists, as well as residents. During three months of inclusion, we only missed 2 patients because of admission during the weekend. All other patients' ONSD could be measured on the first three days after cardiac arrest if still adequately sedated or comatose.

### Trends over time

We calculated the percentage change of the ONSD over time. We found no significant differences between patients with good and poor neurological recovery for changes of ONSD between day 1 and 2, day 1 and day 3, or day 2 and day 3. Although no significant differences in changes over time were found, patients with poor neurological outcome had lower ONSD values on day three than patients with good neurological outcome. Patients with good neurological outcome show a stable ONSD, while

patients with poor neurological recovery show a clear decrease in ONSD during the first three days after resuscitation (figure 3.2). When looking into the changes of ONSD over time for individual patients, we see that patients with good and poor neurological outcome show increases and decreases in ONSD (appendix G).

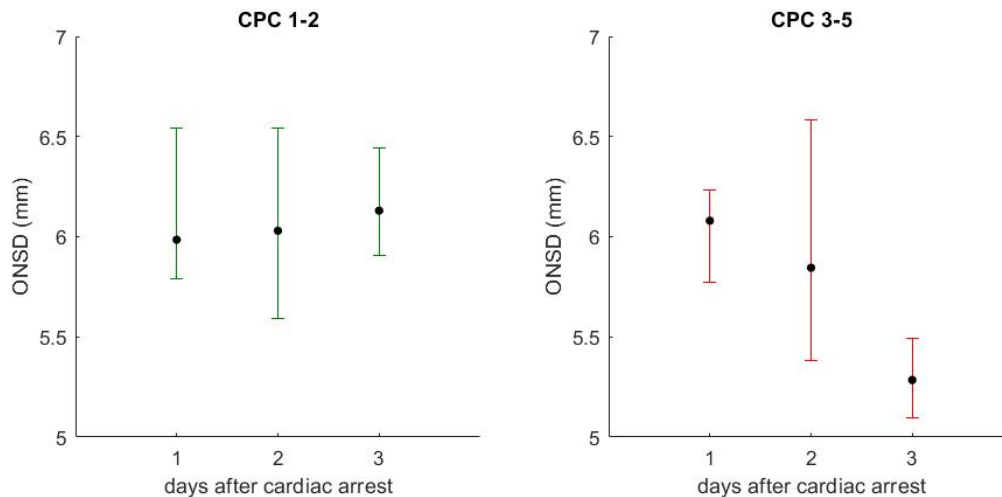


FIGURE 3.2 TREND OVER TIME OF ONSD MEASUREMENTS FOR PATIENTS WITH GOOD NEUROLOGICAL OUTCOME (LEFT) AND POOR NEUROLOGICAL OUTCOME (RIGHT). DATA ARE PRESENTED AS MEDIAN (DOT) AND INTERQUARTILE RANGE (ERROR BARS).

### 3.3 DISCUSSION

With this prospective pilot study, including 11 patients in Rijnstate hospital, we could not replicate previously published findings on associations between ONSD and neurological outcome after cardiac arrest. This indicates that the predictive value of repeated ONSD measurements by ultrasound during the first three days after resuscitation in comatose patients remains unclear.

Measurements can be performed easier and faster than measurements using CT or MRI. Furthermore, ultrasound is cheap and can be performed bedside, and does therefore not require patient transport. Previous research showed a good agreement between ONSD measurements on CT or MRI and using ultrasound [45, 46].

We did not lose any patients due to other reasons than death or awakening. However, at day 3 after resuscitation we only measured 2 patients with poor neurological outcome and 4 patients with good neurological recovery. Therefore, analyses of the measurements on day 3 are not generalizable and inclusion of more patients is needed.

We expected patients with poor neurological outcome to show higher values for ONSD than patients with good neurological outcome during the first three days after resuscitation. Patients with extensive brain damage often develop brain oedema or loss of cerebrovascular pressure reactivity resulting in increased intravascular blood volume. Both phenomena can increase ICP [47]. The sheath surrounding the optic nerve is in continuation with the dura mater of the brain and the subarachnoid interspace. Therefore, high ICP is correlated with measurements of the ONSD [31-33, 44, 48, 49]. However, we showed that no significant differences were present for ONSD measurements on day 1 and day 2

between patients with good and poor neurological outcome. Therefore, poor outcome could only be predicted with very low sensitivity.

At day 3, patients with good neurological outcome had significant higher ONSD measurements than patients with poor neurological outcome. This is in contrast with our hypothesis that patients with poor neurological outcome would have higher larger ONSD than patients with good neurological outcome. This finding can be explained by the small number of patients with ONSD measurements available at day 3 after cardiac arrest. Prediction of outcome based on measurements on day 3 was therefore not performed.

Previous research (n=36) showed significant higher ONSD in patients with poor neurological outcome compared to patients with good neurological outcome at day 1, but no significant differences on day 2 and 3 [28]. Another study (n=17) showed significant higher ONSD in patients with poor neurological outcome than in patients with good neurological outcome measured 12-72 hours after cardiac arrest [30]. However, in this research each patient was only measured once in this time period.

The intra-rater reliability of the measurements is acceptable (78%). This might be explained by the subjectivity of ultrasonography. Large standard deviations can influence our measurements, because of the rather small expected differences between patients with good and poor neurological outcome. To decrease the chance on large standard deviations beforehand, we instructed all researchers on probe movement and how to determine the boundaries of the ONSD during ultrasonography. Intra-rater reliability might be increased by checking the boundaries we set during measurements afterwards on the saved images.

We cannot evaluate the interrater reliability of our measurements because measurements were always performed by one rater. We therefore do not know what the influence of interrater variability on our measurements is. Manually checking the boundaries afterwards on the saved images by one rater could decrease the effects of interrater variability on our measurements.

During the first three days after resuscitation, median ONSD in patients with good neurological outcome remained stable. Median ONSD in patients with poor neurological outcome decreased during the first 3 days. This is not in accordance with previous literature that showed that ONSD decreased in patients with good neurological outcome and increased in patients with poor outcome [28]. However, our findings are based on only 2 and 4 patients with poor neurological outcome on day 2 and 3, respectively.

ONSD in patients with both good and poor neurological outcome can increase and decrease during the first three days after resuscitation. We can therefore not conclude that a decrease or increase of ONSD is predictive for either good or poor neurological outcome.

The most important limitation of this study is the number of patients included. We were only able to include 11 patients in this analysis, of whom 6 had ONSD measurements available at day 3 after cardiac arrest. To increase the reliability of our data, more patients should be included.

Ultrasonographic measurements are subject to interrater and intra-rater variability. Especially in the data we are collecting, small differences in measurements can significantly influence our analyses.

Measurements could be performed at day 1 for every patient, but not for all patients on day 2 and 3. Therefore, we cannot tell whether repeated measurements or measurements later than day 1 could improve outcome prediction in comatose cardiac arrest patients.

### 3.4 CONCLUSION

In our study, the value of ultrasonographic measurements of the ONSD at day 1 to 3 after cardiac arrest to predict neurological outcome was limited. Measurements were cheap, easy and quick with an excellent internal consistency. For definitive conclusions, more patients are needed.



## CHAPTER 4

### GENERAL CONCLUSION AND FUTURE DIRECTIONS

In this thesis, we evaluated the predictive value of continuous EEG, brain MRI and ultrasonographic measurements of the ONSD for prediction of good and poor outcome in comatose patients after cardiac arrest. In chapter 2 we showed that the DGN score, cortex score and proportion of brain with ADC value below  $450 \times 10^{-6} \text{ mm}^2/\text{s}$  add most to neurological outcome prediction based on EEG analysis. Although we only based our results on 30 patients, these results are very promising.

Ultrasonographic measurement of the ONSD was only performed in 11 patients (chapter 3) and our results do not show relevant predictive value, yet. However, inclusion of patients is ongoing. After inclusion of 20 patients, we will evaluate whether the ONSD is likely to add to outcome prediction and decide on (dis)continuation of this ultrasonographic study.

#### FUTURE DIRECTIONS

Most previous studies on outcome prediction after cardiac arrest focus on single predictors. Multimodal prediction models are scarce. This thesis showed the potential of several MRI parameters to add to EEG measures for prediction of good or poor neurological outcome after cardiac arrest. Due to the small numbers of patients included, the robustness and generalizability of our results are still small. Furthermore, we did not include any demographic, biochemical or clinical measures in our predictions. After inclusion of more patients, we aim for internal and external validation of predictive values. Eventually, machine learning techniques may be used to establish optimal prediction models including combinations of demographic, biochemical, clinical, EEG, and MRI measures to best predict good or poor neurological outcome after cardiac arrest. The added value of MRI measures can then be further established.

Until now, we only evaluated quantitative MRI measures based on ADC values of the whole brain, grey matter and white matter. However, visual MRI analysis showed that differences between patients with good and poor neurological outcome are mainly visible in the deep grey nuclei and cerebral cortex. The added value of segmentation of ADC maps into deep grey nuclei and cerebral cortex should therefore be further investigated.

Some patients with poor neurological outcome have a normal EEG and normal structural MRI scan. These patients have brain damage that cannot be detected with these methods. We also collect DTI and fMRI data. DTI can be used to investigate the change of anisotropic movement of water molecules as a result of damage to white matter tracts. Analysis of fMRI can be used to explore activity in brain regions, including the degree of synchronicity. These measures could help distinguish more patients with poor neurological outcome from patients with good neurological outcome [50-53]. Analysis of these data is ongoing.

Before implementation of MRI scans on day 2-4 after cardiac arrest in clinical practice, we should weigh up the benefits against the costs and efforts. Performing MRI scans of comatose patients after cardiac

arrest costs a lot of time, money, and effort from nurses and physicians. Also, there is a potential risk in hemodynamically unstable patients. The patient must be transported to the radiology department and equipment used on the ICU cannot enter the MRI room. Performing MRI scans of these patients is therefore only worth the effort if MRI analysis adds substantially to neurological outcome prediction of patients after cardiac arrest.

This research only focussed on the prediction of outcome based on the CPC score at 6 or 3 months after cardiac arrest. CPC is a rough estimate of functional recovery. Cognitive outcome, depression, and quality of life are more distinguished measures, that may allow further discrimination between good and poor recovery [54]. We follow patients up to 12 months after cardiac arrest and collect data on mental wellbeing, as well. Association between MRI findings and cognitive or emotional disturbances may increase our understanding of the problems patients deal with after cardiac arrest.

If our pilot study will indicate that ONSD measurements are likely to add to outcome prediction, we will study the added value of ONSD measurements in addition to demographic, biochemical, clinical, EEG, and MRI measures in a multimodal prediction model, as well.

## CONCLUSION

Visual and quantitative analysis of brain DWI and FLAIR MRI performed on day 2-4 after cardiac arrest hold potential to increase sensitivity for prediction of good or poor neurological outcome, with equal reliability. Before implementation of MRI scans after cardiac arrest into clinical practice, the additional value on top of demographic, biochemical, clinical, and EEG measures should be investigated based on more patients. We are currently increasing our sample size for multimodal prediction modeling. Furthermore, the additional value should be weighed up against the costs and efforts needed to perform these MRI scans.

We could not replicate previously described predictive values of ultrasonographic measurements of the ONSD, yet, but our current sample size is small. After inclusion of 20 patients, we will decide whether further research into the additional value of ONSD measurements is useful.

## BIBLIOGRAPHY

1. Berdowski, J., et al., *Global incidences of out-of-hospital cardiac arrest and survival rates: Systematic review of 67 prospective studies*. Resuscitation, 2010. **81**(11): p. 1479-1487.
2. Hofmeijer, J., et al., *Early EEG contributes to multimodal outcome prediction of postanoxic coma*. Neurology, 2015. **85**(2): p. 137-143.
3. Bernard, S.A., et al., *Treatment of comatose survivors of out-of-hospital cardiac arrest with induced hypothermia*. New England Journal of Medicine, 2002. **346**(8): p. 557-563.
4. Rundgren, M., et al., *Continuous amplitude-integrated electroencephalogram predicts outcome in hypothermia-treated cardiac arrest patients*. Critical Care Medicine, 2010. **38**(9): p. 1838-1844.
5. Asgari, S., et al., *Quantitative measures of EEG for prediction of outcome in cardiac arrest subjects treated with hypothermia: a literature review*. Journal of Clinical Monitoring and Computing, 2018. **32**(6): p. 977-992.
6. Irisawa, T., et al., *Duration of coma in out-of-hospital cardiac arrest survivors treated with targeted temperature management*. Annals of Emergency Medicine, 2016. **69**(1): p. 36-43.
7. Sekhon, M.S., P.N. Ainslie, and D.E. Griesdale, *Clinical pathophysiology of hypoxic ischemic brain injury after cardiac arrest: a "two-hit" model*. Critical Care, 2017. **21**(90).
8. Ramiro, J.I. and A. Kumar, *Updates on management of anoxic brain injury after cardiac arrest*. Missouri Medicine, 2015. **112**(2): p. 136-141.
9. Federatie Medisch Specialisten, *Prognose van postanoxisch coma*. 2019.
10. Sandroni, C., et al., *Prognostication in comatose survivors of cardiac arrest: an advisory statement from the European Resuscitation Council and the European Society of Intensive Care Medicine*. Resuscitation, 2014. **85**(12): p. 1779-89.
11. Sandroni, C., S. D'Arrigo, and J.P. Nolan, *Prognostication after cardiac arrest*. Critical Care, 2018. **22**(150).
12. Sondag, L., et al., *Early EEG for outcome prediction of postanoxic coma: prospective cohort study with cost-minimization analysis*. Critical Care, 2017. **21**(111).
13. Ruijter, B.J., et al., *The prognostic value of discontinuous EEG patterns in postanoxic coma*. Clinical Neurophysiology, 2018. **129**(8): p. 1534-1543.
14. Ruijter, B.J., et al., *Early electroencephalography for outcome prediction of postanoxic coma: a prospective cohort study*. Annals of Neurology, 2019. **86**(2): p. 203-214.
15. Tjepkema-Cloostermans, M.C., et al., *Cerebral Recovery Index: reliable help for prediction of neurologic outcome after cardiac arrest*. Critical care medicine, 2017. **45**(8): p. e789-e797.
16. Hirsch, K.G., et al., *Multi-center study of diffusion weighted imaging in coma after cardiac arrest*. Neurocritical Care, 2016. **24**(1): p. 82-89.
17. Choi, S.P., et al., *Diffusion-weighted magnetic resonance imaging for predicting the clinical outcome of comatose survivors after cardiac arrest: a cohort study*. Critical Care, 2010. **14**: p. R17.
18. Moon, H.K., et al., *Quantitative analysis of relative volume of low apparent diffusion coefficient value can predict neurologic outcome after cardiac arrest*. Resuscitation, 2018. **126**: p. 36-42.
19. Wallin, E., et al., *Acute brain lesions on magnetic resonance imaging in relation to neurological outcome after cardiac arrest*. Acta Anaesthesiologica Scandinavica, 2017. **62**(5): p. 635-647.
20. Wijman, C.A.C., et al., *Prognostic value of brain diffusion weighted imaging after cardiac arrest*. Annals of Neurology, 2009. **65**(4): p. 394-402.
21. Wu, O., et al., *Comatose patients with cardiac arrest: predicting clinical outcome with diffusion-weighted MR imaging*. Radiology, 2009. **252**(1): p. 173-181.

22. Youn, C.S., et al., *Repeated diffusion weighted imaging in comatose cardiac arrest patients with therapeutic hypothermia*. Resuscitation, 2015. **96**: p. 1-8.
23. Järnum, H., et al., *Diffusion and perfusion MRI of the brain in comatose patients treated with mild hypothermia after cardiac arrest: a prospective observational study*. Resuscitation, 2009. **80**(4): p. 425-430.
24. Ryoo, S.M., et al., *Predicting outcome with diffusion-weighted imaging in cardiac arrest patients receiving hypothermia therapy: multicenter retrospective cohort study*. Critical Care Medicine, 2015. **43**(11): p. 2370-2377.
25. Bevers, M.B., et al., *Combination of clinical exam, MRI and EEG to predict outcome following cardiac arrest and targeted temperature management*. Neurocritical Care, 2018. **29**(3): p. 396-403.
26. Mettenburg, J.M., et al., *Discordant observation of brain injury by MRI and malignant electroencephalography patterns in comatose survivors of cardiac arrest following therapeutic hypothermia*. American Journal of Neuroradiology, 2016. **37**(10): p. 1787-1793.
27. Barth, R., et al., *Topography of MR lesions correlates with standardized EEG pattern in early comatose survivors after cardiac arrest*. Resuscitation, 2020.
28. Chelly, J., et al., *The optic nerve sheath diameter as a useful tool for early prediction of outcome after cardiac arrest: a prospective pilot study*. Resuscitation, 2016. **103**: p. 7-13.
29. Kim, Y.H., et al., *Feasibility of optic nerve sheath diameter measured on initial brain computed tomography as an early neurologic outcome predictor after cardiac arrest*. Academic Emergency Medicine, 2014. **21**(10): p. 1121-8.
30. Ueda, T., et al., *Sonographic optic nerve sheath diameter: a simple and rapid tool to assess the neurologic prognosis after cardiac arrest*. Journal of Neuroimaging, 2015. **25**(6): p. 927-930.
31. Geeraerts, T., et al., *Ultrasonography of the optic nerve sheath may be useful for detecting raised intracranial pressure after severe brain injury*. Intensive Care Medicine, 2007. **33**(10): p. 1704-1711.
32. Jeon, J.P., et al., *Correlation of optic nerve sheath diameter with directly measured intracranial pressure in Korean adults using bedside ultrasonography*. PLoS ONE, 2017. **12**(9): p. e0183170.
33. Rajajee, V., et al., *Optic nerve ultrasound for the detection of raised intracranial pressure*. Neurocritical Care, 2011. **15**(3): p. 506-515.
34. Tjepkema-Cloostermans, M.C., et al., *Predicting outcome in postanoxic coma: are ten EEG electrodes enough?* Journal of Clinical Neurophysiology, 2017. **34**(3): p. 207-212.
35. Hirsch, K.G., et al., *Prognostic value of a qualitative brain MRI scoring system after cardiac arrest*. Journal of Neuroimaging, 2015. **25**(3): p. 430-437.
36. Kitamura, G., et al., *Hypoxic-ischemic injury: utility of susceptibility-weighted imaging*. Pediatric Neurology, 2011. **45**(4): p. 220-224.
37. SPM12. 2014, The Wellcome Centre for Human Neuroimaging, UCL Queen Square Institute of Neurology: London, UK.
38. Mlynash, M., et al., *Temporal and spatial profile of brain diffusion-weighted MRI after cardiac arrest*. Stroke, 2010. **41**(8): p. 1665-1672.
39. Wijdicks, E.F.M., N.G. Campeau, and G.M. Miller, *MR Imaging in Comatose Survivors of Cardiac Resuscitation*. American Journal of Neuroradiology, 2001. **22**(8): p. 1561-1565.
40. Gutierrez, L.G., et al., *CT and MR in non-neonatal hypoxic-ischemic encephalopathy: radiological findings with pathophysiological correlations*. Neuroradiology, 2010. **52**(11): p. 949-976.
41. Busl, K.M. and D.M. Greer, *Hypoxic-ischemic brain injury: pathophysiology, neuropathology and mechanisms*. Neurorehabilitation, 2010. **26**(1): p. 5-13.
42. Geocadin, R.G., et al., *Management of brain injury after resuscitation from cardiac arrest*. Neurologic Clinics, 2008. **26**(2): p. 487-506, ix.

43. Nolan, J.P., et al., *Post-cardiac arrest syndrome: epidemiology, pathophysiology, treatment, and prognostication*. Resuscitation, 2008. **79**(3): p. 350-79.
44. Tjahjadi, N.S., et al., *Point-of-care ultrasound of optic nerve sheath diameter to detect elevated intracranial pressure: ultrasound in the eye of the beholder?* Netherlands Journal of Critical Care, 2019. **27**(2): p. 81-86.
45. Hassen, G.W., et al., *Accuracy of optic nerve sheath diameter measurement by emergency physicians using bedside ultrasound*. Ultrasound in Emergency Medicine, 2015. **48**(4): p. 450-457.
46. Shirodkar, C.G., et al., *Correlation of measurement of optic nerve sheath diameter using ultrasound with magnetic resonance imaging*. Indian Journal of Critical Care Medicine, 2015. **19**: p. 466-70.
47. Elmer, J., *Prognosis at the speed of sound: measuring optic nerve sheath diameter after cardiac arrest*. Resuscitation, 2019. **143**: p. 217-218.
48. Kimberly, H.H., et al., *Correlation of optic nerve sheath diameter with direct measurement of intracranial pressure*. Academic Emergency Medicine, 2008. **15**(2): p. 201-204.
49. Robba, C., et al., *Optic nerve sheath diameter measures sonographically as non-invasive estimator of intracranial pressure: a systematic review and meta-analysis*. Intensive Care Medicine, 2018. **44**(8): p. 1284-1294.
50. Koenig, M.A., et al., *MRI default network connectivity is associated with functional outcome after cardiopulmonary arrest*. Neurocritical Care, 2014. **20**(3): p. 348-357.
51. Sair, H.I., et al., *Early functional connectome integrity and 1-year recovery in comatose survivors of cardiac arrest*. Radiology, 2017. **287**(1): p. 247-255.
52. Luyt, C.-E., et al., *Diffusion tensor imaging to predict long-term outcome after cardiac arrest - A bicentric pilot study*. Anesthesiology, 2012. **117**(6): p. 1311-1321.
53. Eerden, A.W.v.d., et al., *White matter changes in comatose survivors of anoxic ischemic encephalopathy and traumatic brain injury: comparative diffusion-tensor imaging study*. Neuroradiology, 2014. **270**(2): p. 506-516.
54. Moulart, V.R.M.P., et al., *Cognitive impairments in survivors of out-of-hospital cardiac arrest: a systematic review*. Resuscitation, 2009. **80**(3): p. 297-305.
55. Hofmeijer, J. and M.J.A.M.v. Putten, *Ischemic cerebral damage: an appraisal of synaptic failure*. Stroke, 2012. **43**(2): p. 607-615.
56. Bolay, H., et al., *Persistent defect in transmitter release and synapsin phosphorylation in cerebral cortex after transient moderate ischemic injury*. Stroke, 2002. **33**(5): p. 1369-75.
57. Keijzer, H.M., et al., *Brain imaging in comatose survivors of cardiac arrest: pathophysiological correlates and prognostic properties*. Resuscitation, 2018. **133**: p. 124-136.
58. Ruijter, B.J., M.J.A.M.v. Putten, and J. Hofmeijer, *Generalized epileptiform discharges in postanoxic encephalopathy: quantitative characterization in relation to outcome*. Epilepsia, 2015. **56**(11): p. 1845-54.
59. Tjepkema-Cloostermans, M.C., et al., *Generalized periodic discharges after acute cerebral ischemia: reflection of synaptic failure?* Clinical Neurophysiology, 2014. **125**(2): p. 244-262.
60. Dijkstra, K., et al., *A biophysical model for cytotoxic cell swelling*. The Journal of Neuroscience, 2016. **36**(47): p. 11881-11890.
61. Kummer, R.v. and I. Dzialowski, *Imaging of cerebral ischemic edema and neuronal death*. Neuroradiology, 2017. **59**(6): p. 545-553.
62. Ajam, K., et al., *Reliability of the Cerebral Performance Category to classify neurological status among survivors of ventricular fibrillation arrest: a cohort study*. Scandinavian Journal of Trauma, Resuscitation and Emergency Medicine, 2011. **19**(38).
63. Fried, S. and S.L. Moshé, *Basic physiology of the EEG*. Neurology Asia, 2011. **16**: p. 23-25.

64. Bandyopadhyay, S., M.Z. Koubeissi, and N.J. Azar, *Psychologic basis of EEG and epilepsy*, ed. Epilepsy Board Review. 2017, New York: Springer.
65. St. Louis, E.K. and L.C. Frey, *Electroencephalography (EEG): an introductory test and atlas of normal and abnormal findings in adults, children and infants*. 2016, Chicago: American Epilepsy Society.
66. Cloostermans, M.C., et al., *Continuous electroencephalography monitoring for early prediction of neurological outcome in postanoxic patients after cardiac arrest: a prospective cohort study*. *Critical Care Medicine*, 2012. **40**(10): p. 2867-2875.
67. Rossetti, A.O., A.A. Rabinstein, and M. Oddo, *Neurological prognostication of outcome in patients in coma after cardiac arrest*. *Lancet Neurology*, 2016. **15**(6): p. 597-609.
68. Sivaraju, A., et al., *Prognostication of post-cardiac arrest coma: early clinical and electroencephalographic predictors of outcome*. *Intensive Care Medicine*, 2015. **41**(7): p. 1264-1272.
69. Soholm, H., et al., *Prognostic value of electroencephalography (EEG) after out-of-hospital cardiac arrest in successfully resuscitated patients used in daily clinical practice*. *Resuscitation*, 2014. **85**(11): p. 1580-1585.
70. Tjepkema-Cloostermans, M.C., et al., *Electroencephalogram predicts outcome in patients with postanoxic coma during mild therapeutic hypothermia*. *Critical Care Medicine*, 2015. **43**(1): p. 159-67.
71. Tjepkema-Cloostermans, M.C., et al., *A Cerebral Recovery Index (CRI) for early prognosis in patients after cardiac arrest*. *Critical Care*, 2013. **17**(5): p. R252.
72. Blink, E.J., *MRI principes - voor iedereen die geen graag in fysica heeft*. 2004.
73. Grover, V.P.B., et al., *Magnetic Resonance Imaging: principles and techniques: lessons for clinicians*. *Journal of Clinical and Experimental Hepatology*, 2015. **5**(3): p. 246-255.
74. Le Bihan, D. and M. Lima, *Diffusion Magnetic Resonance Imaging: what water tells us about biological tissues*. *PLoS Biology*, 2015. **13**(7): p. e1002203.
75. Le Bihan, D. and H. Johansen-Berg, *Diffusion MRI at 25: exploring brain tissue structure and function*. *Neuroimage*, 2012. **61**(2): p. 324-341.
76. Verma, A. and U. Bashir. *Diffusion weighted imaging*. 2019-12-10]; Available from: <https://radiopaedia.org/articles/diffusion-weighted-imaging-1>.
77. Bell, D.J. and A. Goel. *B values*. 2019-12-10]; Available from: <https://radiopaedia.org/articles/b-values-1>.
78. Le Bihan, D., *Apparent diffusion coefficient and beyond: what diffusion MR imaging can tell us about tissue structure*. *Radiology*, 2013. **268**(2): p. 318-322.
79. Reimer, P., et al., *Clinical MR imaging: a practical approach*. 2010: Springer Science & Business Media. 820.
80. De Coene, B., et al., *MR of the brain using fluid-attenuated inversion recovery (FLAIR) pulse sequences*. *American Journal of Neuroradiology*, 1992. **13**: p. 1555-1564.
81. Adams, J.G. and E.R. Melhem, *Clinical usefulness of T2-weighted fluid-attenuated inversion recovery MR imaging of the CNS*. *American Journal of Roentgenology*, 1998. **172**: p. 529-536.
82. Haacke, E.M., et al., *Susceptibility weighted imaging: technical aspects and clinical applications, part 1*. *American Journal of Neuroradiology*, 2009. **30**(1): p. 19-30.
83. Halefoglu, A.M. and D.M. Yousem, *Susceptibility weighted imaging: clinical applications and future directions*. *World Journal of Radiology*, 2018. **10**(4): p. 30-45.
84. Gasparotti, R., L. Pinelli, and R. Liserre, *New MR sequences in daily practice: susceptibility weighted imaging. A pictorial essay*. *Insights Imaging*, 2011. **2**(3): p. 335-347.
85. Robba, C., et al., *Brain ultrasonography: methodology, basic and advanced principles and clinical applications. A narrative review*. *Intensive Care Medicine*, 2019. **45**(7): p. 913-927.

# APPENDICES

## APPENDIX A - GENERAL BACKGROUND

### A.1 Postanoxic encephalopathy

Postanoxic encephalopathy is the primary cause of death in comatose patients after cardiac arrest. Within 20 seconds after cardiac arrest, patients lose consciousness due to a cessation of cerebral circulation [7, 8]. The earliest consequences of cerebral ischemia are changes in synaptic neurotransmission resulting from presynaptic malfunction with impaired transmitter release [55, 56]. Excitatory synapses to inhibitory interneurons are likely to be more vulnerable to hypoxia than inhibitory synapses, resulting in characteristic EEG patterns and status myoclonus [57-59].

Decrease of oxygen delivery to the brain results in the halt of adenosine triphosphate (ATP) production. The decreased ATP production causes malfunctioning of the energy-dependent sodium-potassium pumps in the neuronal and glial plasma membrane. Consequently, transmembrane ionic gradients can not be maintained and influx of sodium and chloride into the intracellular space occurs. Due to the decreased extracellular sodium, intravascular sodium, chloride and water molecule will be transported into the extracellular space resulting in cerebral cytotoxic oedema [60, 61]. Blood-brain-barrier breakdown causes leakage of plasma proteins into the extracellular space. This leads to an increase in extracellular water and therefore vasogenic oedema [61]. Both cytotoxic and vasogenic oedema cause the brain tissue to swell which can further decrease cerebral perfusion pressure.

Beside cerebral oedema, cerebral lactate accumulation, intracellular acidosis and glutamate release can induce neuronal cell damage and tissue breakdown [7, 41].

Brain structures most susceptible to postanoxic damage are the hippocampus, thalamus, striatum, neocortex and Purkinje cells of the cerebellum [7, 8, 40, 41].

### A.2 Neurological outcome after cardiac arrest

An often used measure for describing neurological outcome after cardiac arrest is the Cerebral Performance Category (CPC) score [11]. CPC 1 represents the best possible outcome while CPC 5 represents (brain) death. Table A.1 shows all possible CPC scores and corresponding descriptions. Generally, CPC 1 and 2 are classified as a good neurological outcome, CPC 3-5 as a poor neurological outcome.

TABLE A.1 CEREBRAL PERFORMANCE CATEGORY [62]

<b>CPC 1</b>	Good clinical performance ( <i>normal life</i> )	Conscious, alert, able to work and lead a normal life. May have minor psychological or neurologic deficits (mild dysphasia, nonincapacitating hemiparesis, or minor cranial nerve abnormalities).
<b>CPC 2</b>	Moderate cerebral disability ( <i>disabled, but independent</i> )	Conscious. Sufficient cerebral function for part-time work in sheltered environment or independent activities of daily life (dress, travel by public transportation, food preparation). May have hemiplegia, seizures, ataxia, dysarthria, dysphasia, or permanent memory or mental changes.
<b>CPC 3</b>	Severe cerebral disability ( <i>conscious, but disabled and dependent</i> )	Conscious; dependent on others for daily support (in an institution or at home with exceptional family effort). Has at least limited cognition. This category includes a wide range of cerebral abnormalities, from patients who are ambulatory but have severe memory disturbances or dementia precluding independent existence to those who are paralyzed and can communicate only with their eyes, as in the locked-in syndrome.
<b>CPC 4</b>	Coma/vegetative state ( <i>unconscious</i> )	Unconscious, unaware of surroundings, no cognition. No verbal or psychologic interaction with environment.
<b>CPC 5</b>	Brain death	Certified brain dead or dead by traditional criteria.

### A.3 Outcome prediction nowadays

Outcome prediction of comatose patients after cardiac arrest in the Netherlands is nowadays based on the directive written by the 'Federatie Medisch Specialisten', initiated by the Dutch Neurology Society [9].

#### *Prediction of poor neurological outcome*

A patient's neurological outcome after cardiac arrest might only be predicted if the patient is in a persistent deep coma (at least 24 hours after cardiac arrest) with a motor score of 1 or 2 on the GCS. During GCS evaluation, consciousness should not be affected by sedatives, metabolic disruption or other factors than hypoxic-ischemic brain damage.

Bilateral dilated pupils without light response  $\geq 24$  hours after cardiac arrest, bilateral absent N20 response at median nerve somatosensory evoked potential (SSEP), isoelectric EEG  $\geq 12$  hours after cardiac arrest, low-voltage EEG  $\geq 24$  hours after cardiac arrest, burst-suppression EEG pattern with identical bursts  $\geq 24$  hours after cardiac arrest, or generalized periodic discharges (GPDs) on an isoelectric background pattern  $\geq 24$  hours after cardiac arrest can predict poor neurological outcome with a false positive rate (FPR)  $< 1\%$ .

When none of the test results described above are present after the first 24 hours, another 24 hours should be waited. When the patient's neurologic state does not improve, the tests described above should be repeated.

Neuron specific enolase (NSE) in serum  $>65 \mu\text{g/L}$  48 to 72 hours after cardiac arrest, status myoclonus in the first 48 hours after cardiac arrest or CT brain with diffuse brain oedema in the first week after cardiac arrest are strongly associated with a poor neurological outcome, but are less reliable than the

tests described before (FPR 1-5%). These results should therefore only be used in a multimodal approach.

If none of the described tests gives enough certainty about the prognosis of a patient, recovery should be awaited. The longer a patient remains unconscious, the smaller the chance of a good functional outcome.

#### A.4 Electroencephalography (EEG)

##### *Working mechanism*

Surface electroencephalography (EEG) is a non-invasive measurement of cortical electrical activity. The recorded EEG signal represents the combined postsynaptic potentials of many billions of neurons. This electrical activity is the summation of inhibitory and excitatory postsynaptic potentials (IPSPs and EPSPs) caused by neurotransmitter release from the presynaptic terminals [63-65].

##### *Long-term EEG registrations*

Long-term EEG registrations are used to predict neurological outcome in comatose postanoxic patients. Figure A.1 and A.2 show two different EEG montages used for prediction. Figure A.1 shows the international 10-20 system, whether figure A.2 shows a reduced montage based on research performed by Tjepkema-Cloostermans et al [34].

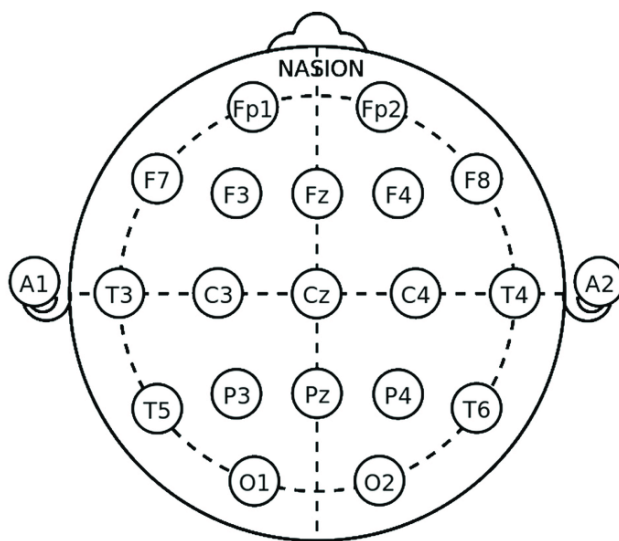


FIGURE A.1 ELECTRODE POSITIONS ACCORDING TO THE INTERNATIONAL 10-20 SYSTEM

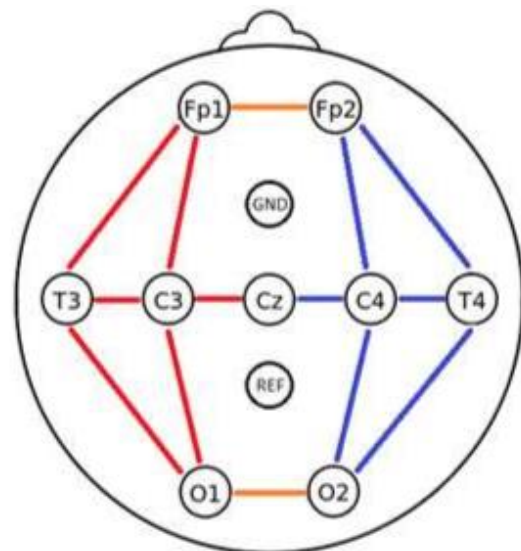


FIGURE A.2 REDUCED MONTAGE WITH 10 ELECTRODES

##### *EEG patterns in comatose patients*

Previous research showed that visual classification of the EEG in comatose patients after cardiac arrest within 24 hours after arrest contributes to neurological outcome prediction. The early recovery of the EEG to a continuous background is a predictor of good neurological outcome. Furthermore, a prolonged

interval of suppressed or synchronous EEG patterns is a specific predictor for poor neurological outcome [2, 12, 14, 66-70].

Prediction of poor neurological outcome based on an unfavourable EEG pattern at 6, 12 and/or 24 hours after cardiac arrest yields a sensitivity of 52% at 100% specificity. Furthermore, a continuous EEG at 6 and/or 12 hours after cardiac arrest predicts good neurological outcome with a sensitivity of 63% at a specificity of 90% [14].

#### *Quantitative EEG measures in comatose patients*

Quantitative EEG features have been evaluated widely in previous research. The continuity of the EEG signal and the amplitude ratio between bursts and suppressions at different times after cardiac arrest have showed good predictive value [13]. A cerebral recovery index has been developed based on the alpha-to-delta ratio, signal power, Shannon entropy, delta coherence and regularity of the EEG signal. This Cerebral Recovery Index showed promising results in the prediction of neurological outcome after cardiac arrest [15, 71].

These quantitative EEG models showed sensitivities of 4 to 59% at 100% specificity for the prediction of poor neurological outcome and sensitivities of 0 to 64% at 90 to 100% specificity for the prediction of good neurological outcome.

## A.5 Magnetic resonance imaging (MRI)

### *Working mechanism*

Magnetic resonance imaging (MRI) is a medical imaging technique based on magnetisation of body protons. A large magnet creates a magnetic field ( $B_0$ ) that aligns protons either parallel or anti-parallel with  $B_0$  in the z-direction. The net magnetisation (the difference between parallel and anti-parallel aligned protons) is used for image formation. The protons spin with a frequency equal to the Larmor frequency, which is related to the magnetic field applied.

The net magnetisation can be manipulated by sending radiofrequency (RF) pulses harmonized with the Larmor frequency of the protons. Magnetized protons absorb the energy during excitation and are flipped to the XY-plane (figure A.3). With time, relaxation takes place and the protons return to the z-direction. During relaxation, protons emit RF pulses. These emitted RF pulses are detected by a coil and Fourier transformed to create an image (figure A.4).

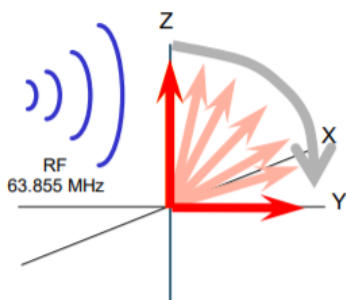


FIGURE A.3 AN EXCITATORY RF PULSE FLIPS THE NET MAGNETIZATION FROM THE Z-DIRECTION TOWARDS THE XY-PLANE [72].

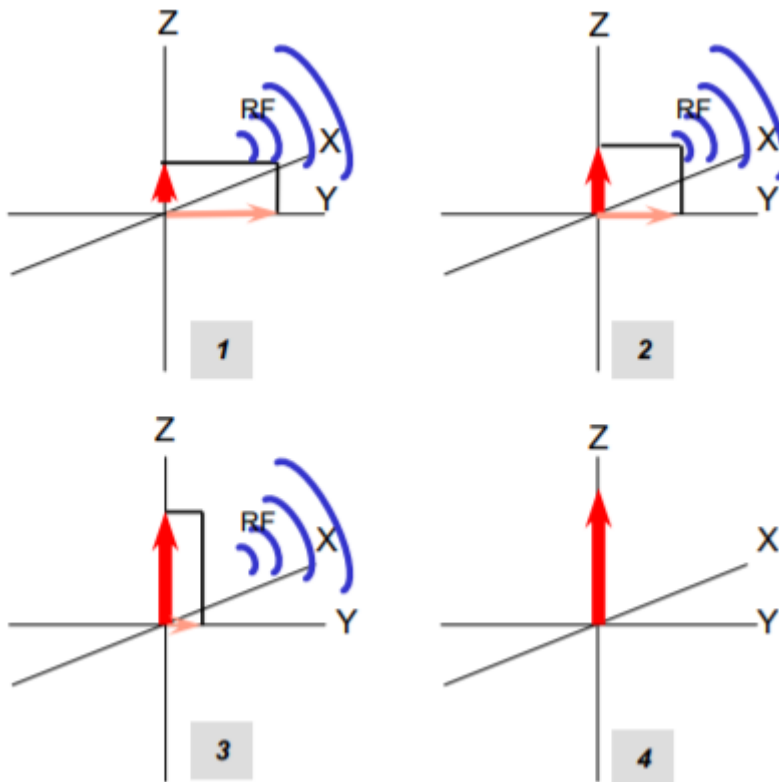


FIGURE A.4 WITH TIME, THE NET MAGNETIZATION RESTORES TOWARDS THE Z-DIRECTION. THE ENERGY RELEASED IS EMITTED AS RF-PULSES [72].

To spatially localise the emitted RF pulses, gradients are used. These are spatially linear variations in the magnetic field, resulting in slightly slower or faster precession and small changes in phase of the protons along the gradient [73, 74].

#### *T1-weighted imaging*

T1-weighted imaging is based on the differences in T1-relaxation times of tissue. Immediately after the RF excitation pulse, the net magnetisation is flipped to the XY-plane. The net magnetisation in Z-direction is therefore 0. Due to T1-relaxation, the net magnetisation slowly returns towards the Z-direction. However, the speed of T1-relaxation is different for all tissues. The percentage of returned net magnetisation in Z-direction at the moment of data acquisition sets the signal intensity of the voxel. T1-weighted sequences have short repetition times and short echo times and are mostly used for detailed anatomic images.

#### *T2-weighted imaging*

T2-weighted imaging is based on the differences in T2-relaxation times of tissue. The RF-excitation pulse aligns all protons to spin in phase with each other. Due to T2-relaxation, protons spin at different speed, resulting in dephasing of the protons. The speed of T2-relaxation is different for all tissues. T2-weighted sequences have longer repetition and echo times. T2-relaxation is a much shorter process than T1-relaxation is.

Differences of intensities of brain structures between T1- and T2-weighted images are shown in table A.2.

TABLE A.2 INTENSITY OF DIFFERENT STRUCTURES ON BRAIN MRI USING T1- AND T2-WEIGHTED IMAGING.

	T1-weighted	T2-weighted
<b>CSF</b>	Dark	Bright
<b>Cortex</b>	Grey	Light grey
<b>White matter</b>	Bright	Dark grey
<b>Fat</b>	Bright	Bright

### *Diffusion weighted imaging (DWI)*

Diffusion weighted imaging (DWI) is based on measuring the random Brownian motion of water molecules within a voxel of tissue. In brain tissue, the microstructure within grey and white matter restricts water molecule movement. Diffusion-driven displacements of the water molecules result in dephasing and an attenuation of the MR signal due to the exposure to varying gradient strengths. Due to this effect, areas with diffusion restriction become hyperintense on the DWI signal, because the signal is less attenuated. A b-value is applied that measures the degree of diffusion weighting applied, based on the amplitude, time and duration between the gradients. The higher the b-value, the more pronounced the diffusion-related signal attenuation. Diffusion-weighted images are affected by T1- and T2-relaxation times. Apparent diffusion coefficient (ADC) maps can be created, which are not susceptible to these relaxation times and are therefore only affected by water diffusivity. ADC is calculated using 2 diffusion weighted images with different b-values using:

$$ADC = \frac{\ln\left(\frac{S_0}{S_1}\right)}{(b_1 - b_0)},$$

where  $S_0$  and  $S_1$  are the signal intensity obtained with the  $b_0$  and  $b_1$  b-values, respectively.

On ADC maps tissues with high diffusion appear white, while tissues with low diffusion appear dark [73, 75-78]. DWI and ADC maps are widely used for imaging of diffusion restriction in the brain, for instance as a result of cytotoxic cerebral oedema [79].

Cytotoxic oedema as a result of PAE causes restriction of water diffusion in the brain. This is visible as hyperintense DWI signal and hypo intensities on the ADC maps. Previous research showed that patients with good neurological outcome show significant higher whole brain ADC values and higher ADC values in specific brain regions than patients with poor neurological outcome do. Furthermore, patients with poor neurological outcome have larger brain volumes below 450 and 650 x 10<sup>-6</sup> mm<sup>2</sup>/s [16-22, 25, 26].

Visual assessment of DWI images showed more diffusion restriction in patients with poor neurological outcome compared to patients with good neurological outcome [17, 19, 23, 24, 35].

*Fluid-attenuated inverse recovery (FLAIR) imaging*

Fluid-attenuated inverse recovery (FLAIR) imaging is used to suppress the high signal of CSF on T2-weighted images. Because the signal of CSF on T2-weighted images is hyperintense compared to the brain it creates artefacts which makes diagnosis of small lesions close to the CSF difficult. FLAIR imaging uses an inversion time that reduces the signal from CSF, but allows the recovery of most of the brain magnetisation [80, 81]. FLAIR imaging facilitates the analysis of brain regions close to CSF, for instance the periventricular spaces. FLAIR imaging is useful for identification of vasogenic oedema in brain regions close to the ventricles, because vasogenic oedema causes hyperintensities on T2 and FLAIR images [79].

Previous research showed that patients with a poor neurological outcome have higher FLAIR ratios (FLAIR signal intensity in grey matter region divided by mean signal intensity of subcortical white matter) in basal ganglia, cortex and putamen [25].

Visual assessment of FLAIR images showed significant more abnormalities in patients with poor neurological outcome compared to patients with good neurological outcome [35].

*Susceptibility weighted imaging (SWI)*

Susceptibility weighted imaging (SWI) is based on the magnetic susceptibility differences of various tissues. Deoxygenated haemoglobin has paramagnetic properties, resulting in field inhomogeneities. Therefore, a phase difference between vessels containing deoxygenated blood and surrounding tissue exists. SWI highlights small changes in susceptibility across a voxel as signal intensity loss. The prominence of cerebral veins on SWI images gives information about the amount of deoxygenated haemoglobin in these veins [36, 82-84]. It is therefore presumed to be an indirect measure of brain metabolism. High prominence of the deep medullary veins is a measure of decreased oxygenated haemoglobin, whereas low prominence of veins indicates an increase of oxygenated haemoglobin.

High prominence of vein scores may be caused by hypoperfusion of brain regions with increased microvascular resistance. Furthermore, ischemia may induce cerebral hypoxia and increased oxygen extraction. Both mechanisms result in a decreased amount of oxygenated haemoglobin, and thus an increased prominence of veins. Low prominence of vein scores might be a result of swelling of the brain, causing compression of the vessels. Furthermore, impaired autoregulation may cause increased perfusion of the damaged brain. Energy failure might result in a lower oxygen extraction. Those mechanisms cause an increased amount of oxygenated haemoglobin in the cerebral circulation, and therefore result in a low prominence of vein score [36].

Previous research showed that patients with a good neurological outcome after hypoxic-ischemic injuries are likely to have SWI images with normal prominence of deep medullary veins (DMVs), whereas patients with a poor neurological outcome are likely to have SWI images with DMVs that are more or less prominent than normal. However, this research has only been performed in neonates that suffered hypoxic-ischemic injury within the first 3 days after birth [36]. No research was found that investigated SWI images of adult patients after cardiac arrest.

## A.6 Optic nerve sheath diameter (ONSD)

The sheath surrounding the optic nerve is in continuation with the subarachnoid space. Therefore, rises in ICP are transmitted to the optic nerve, resulting in swelling of the optic nerve sheath. The anterior part of the optic nerve sheath is more distensible than the posterior part [85]. Therefore, the ONSD can best be measured 3 mm behind the retina. ONSD can be measured using brain CT or MRI or using ocular ultrasound. Ocular ultrasound has the advantage of being cheap and safe, and the ability of being used as a bedside tool.

Several studies showed that ONSD is correlated with ICP [31-33, 48]. The predictive value of ONSD measurements performed on comatose patients after cardiac arrest has also been investigated. Previous studies showed that patients with poor neurological outcome had significant higher ONSD values than patients with good neurological outcome [28-30]. However, the optimal timing of the measurements, the value of repeated measurements, and the optimal cut-off point are still unknown.

## APPENDIX B – EEG ANALYSES

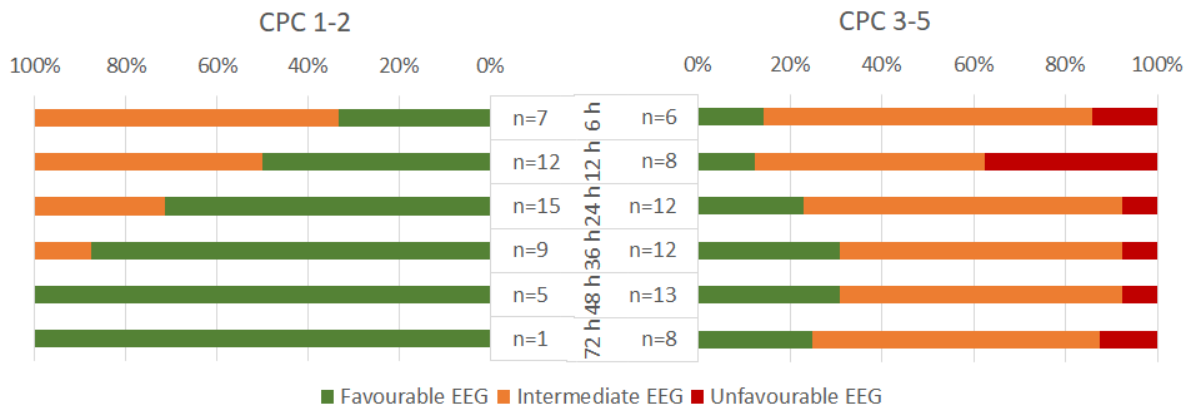


FIGURE B.1 PERCENTAGES OF PATIENTS WITH FAVOURABLE, INTERMEDIATE AND UNFAVOURABLE EEGS BASED ON VISUAL EEG CLASSIFICATION AT 6, 12, 24, 36, 48 AND 72 HOURS AFTER CARDIAC ARREST IN GROUPS WITH GOOD AND POOR NEUROLOGICAL OUTCOME.

APPENDIX C – VISUAL FLAIR AND DWI ANALYSIS

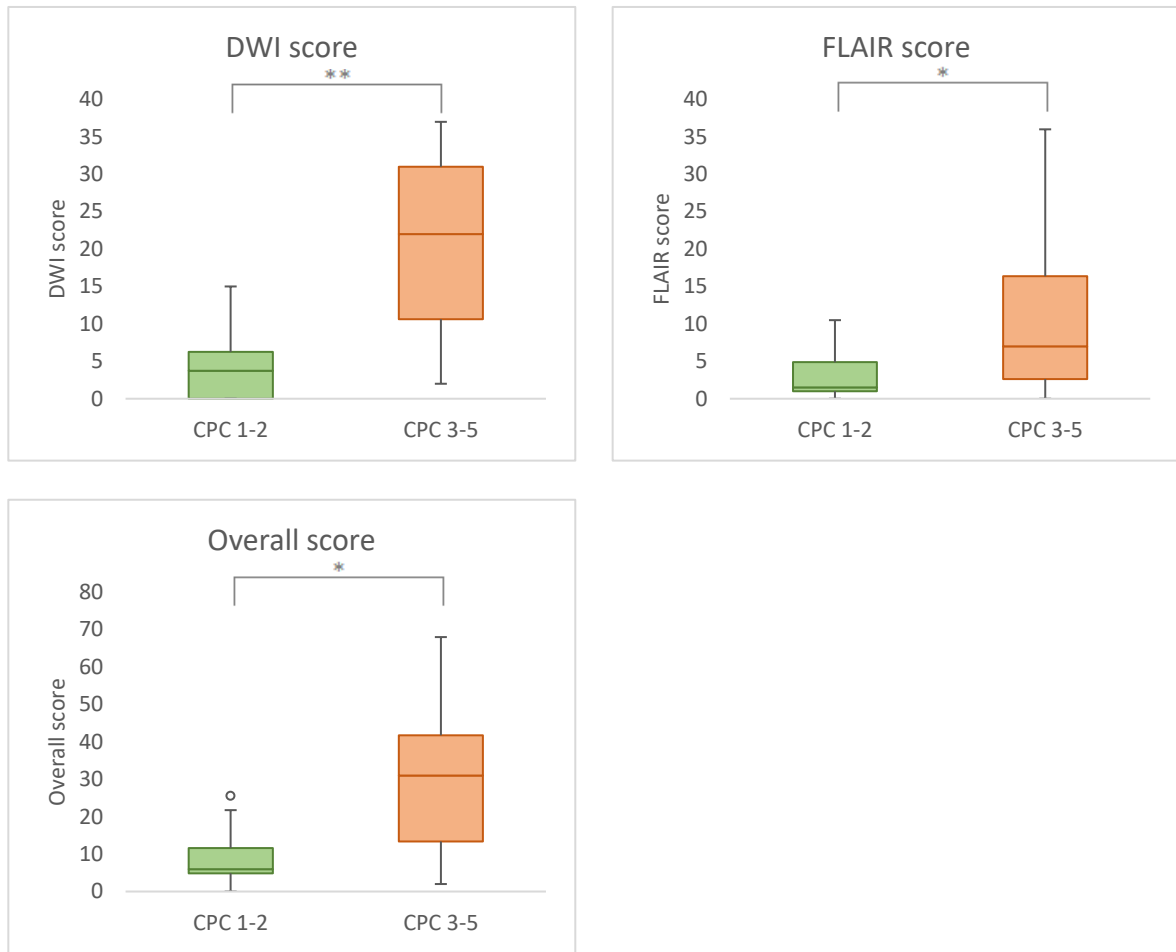


FIGURE C.1 GROUP DIFFERENCES OF THE DWI SCORE, FLAIR SCORE, AND OVERALL SCORE BASED ON VISUAL ANALYSIS OF DWI AND FLAIR SCANS FOR PATIENTS WITH GOOD AND POOR NEUROLOGICAL OUTCOME. ASTERISKS INDICATES A SIGNIFICANT DIFFERENCE ON GROUP LEVEL (\* P<0.05, \*\* P<0.01).

## APPENDIX D – VISUAL SWI ANALYSIS

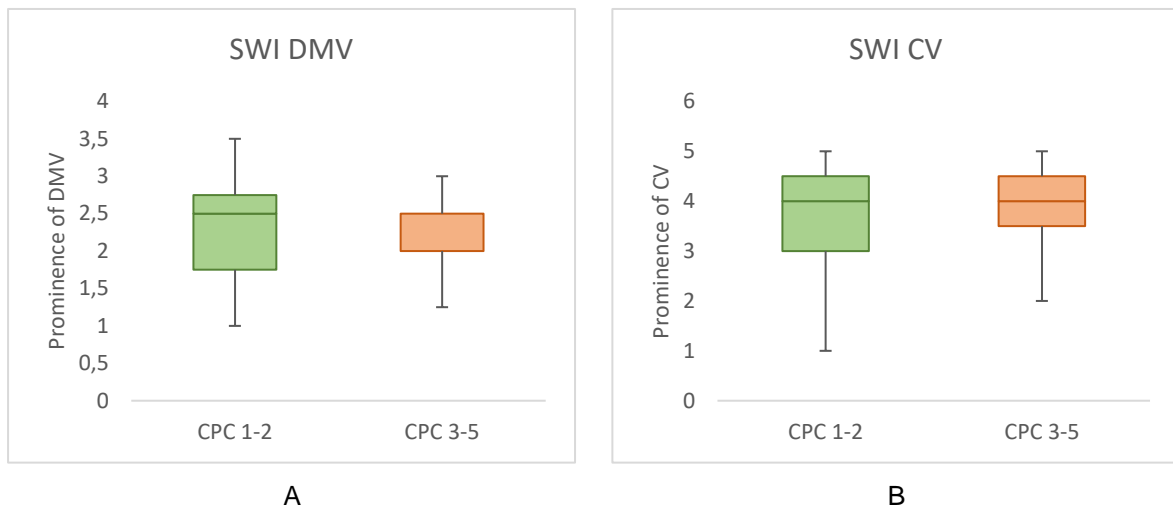


FIGURE D.1 GROUP DIFFERENCES OF VISUAL ANALYSIS OF THE DMVs (A) AND CORTICAL VEINS (B) ON THE SWI BETWEEN PATIENTS WITH GOOD AND POOR NEUROLOGICAL OUTCOME. NO SIGNIFICANT GROUP DIFFERENCES WERE FOUND.

APPENDIX E – QUANTITATIVE MRI ANALYSIS

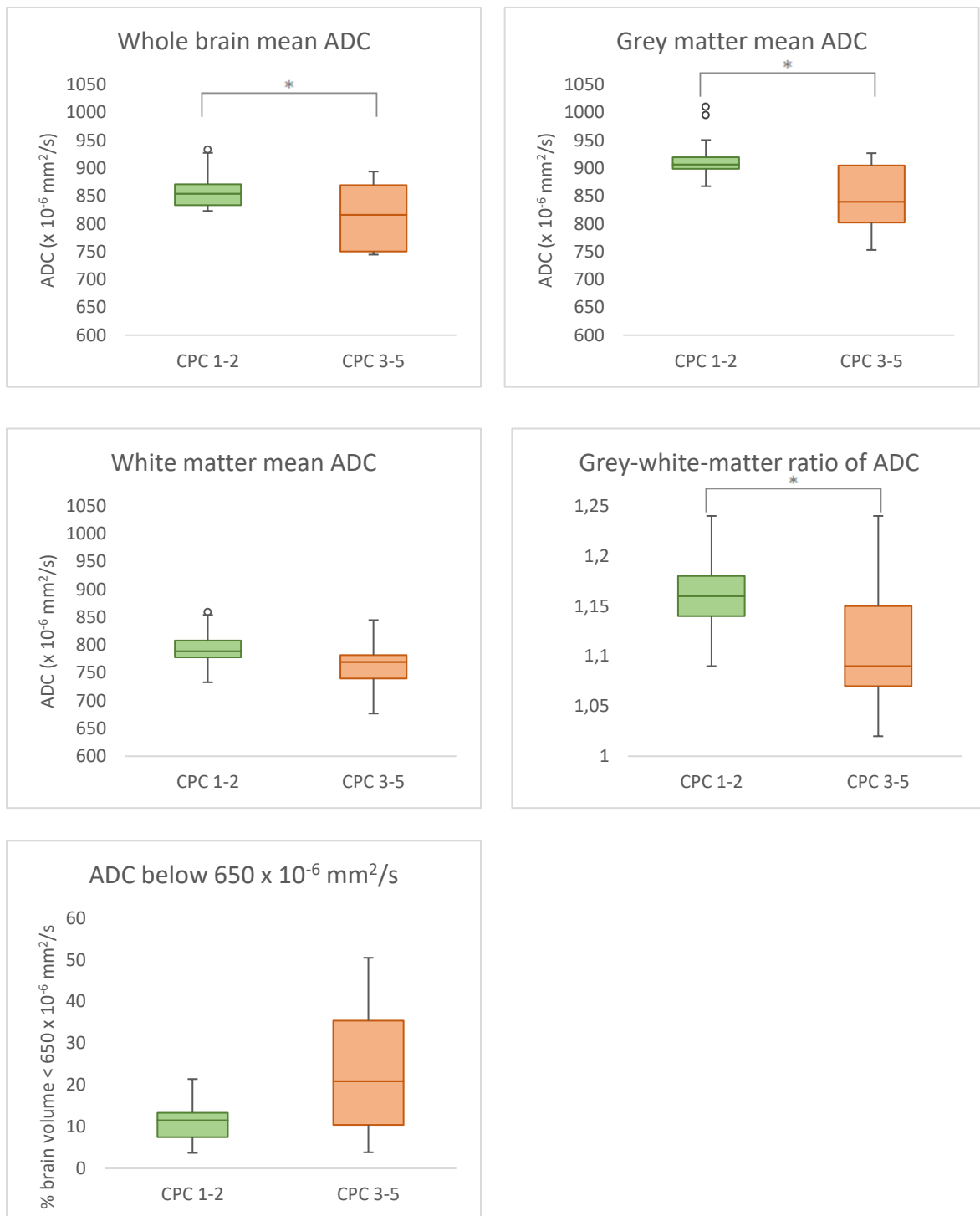


FIGURE E.1 GROUP DIFFERENCES OF FIVE QUANTITATIVE MRI PARAMETERS BETWEEN PATIENTS WITH GOOD AND POOR NEUROLOGICAL OUTCOME. ASTERISKS INDICATE STATISTICALLY SIGNIFICANT DIFFERENCES (\*  $P < 0.05$ ).

## APPENDIX F – CORRELATION BETWEEN EEG AND MRI

TABLE F.1 PEARSON'S CORRELATION COEFFICIENTS REPRESENTING THE CORRELATION BETWEEN EEG PARAMETERS AT VARIOUS TIMEPOINTS AND MRI MEASURES. ASTERISKS INDICATE SIGNIFICANT CORRELATIONS (\* P&lt;0.05, \*\* P&lt;0.01).

	BCI 12h	BCI 24h	BCI 48h	BCI 72h	BSAR 12h	BSAR 24h	BSAR 48h	BSAR 72h
Whole brain ADC	R=0.452 p=0.079	R=0.316 p=0.163	R=0.534 p=0.090	R=-0.083 p=0.875	R=-0.149 p=0.582	R=-0.303 p=0.182	R=0.005 p=0.987	R=0.308 p=0.553
Grey matter ADC	R=0.521 p=0.038*	R=0.449 p=0.041*	R=0.600 p=0.051	R=0.114 p=0.830	R=-0.274 p=0.305	R=-0.369 p=0.099	R=-0.114 p=0.739	R=0.106 p=0.842
White matter ADC	R=0.302 p=0.256	R=0.015 p=0.948	R=0.274 p=0.415	R=-0.413 p=0.416	R=0.087 p=0.749	R=-0.138 p=0.552	R=0.236 p=0.484	R=0.549 p=0.260
Grey-white matter ratio	R=0.378 p=0.149	R=0.544 p=0.011*	R=0.751 p=0.008*	R=0.553 p=0.255	R=-0.501 p=0.048*	R=-0.288 p=0.205	R=-0.494 p=0.123	R=-0.418 p=0.410
% <650 x10 <sup>-6</sup> mm <sup>2</sup> /s	R=-0.573 p=0.020*	R=-0.274 p=0.229	R=-0.533 p=0.091	R=-0.217 p=0.680	R=0.223 p=0.406	R=0.434 p=0.049*	R=-0.074 p=0.830	R=-0.127 p=0.811
% <450 x10 <sup>-6</sup> mm <sup>2</sup> /s	R=-0.612 p=0.012*	R=-0.219 p=0.341	R=-0.661 p=0.027*	R=-0.318 p=0.538	R=0.131 p=0.629	R=0.495 p=0.023*	R=0.132 p=0.699	R=0.370 p=0.470
Cortex score	R=-0.821 p<0.001**	R=-0.556 p=0.009**	R=-0.364 p=0.271	R=-0.725 p=0.103	R=0.164 p=0.544	R=0.230 p=0.317	R=0.302 p=0.367	R=0.542 p=0.267
DGN score	R=-0.527 p=0.036*	R=-0.692 p=0.001**	R=-0.553 p=0.077	R=-0.672 p=0.144	R=0.114 p=0.674	R=0.192 p=0.403	R=0.269 p=0.414	R=0.109 p=0.837
DWI score	R=-0.805 p<0.001**	R=-0.607 p=0.002**	R=-0.644 p=0.033*	R=-0.714 p=0.111	R=0.299 p=0.228	R=0.405 p=0.055	R=0.295 p=0.378	R=0.266 p=0.610
FLAIR score	R=-0.616 p=0.007**	R=-0.518 p=0.011*	R=-0.149 p=0.663	R=-0.730 p=0.099	R=-0.080 p=0.715	R=-0.059 p=0.790	R=0.158 p=0.643	R=0.395 p=0.493
Overall score	R=-0.760 p=0.001**	R=-0.602 p=0.004**	R=-0.437 p=0.179	R=-0.741 p=0.092	R=0.115 p=0.672	R=0.243 p=0.288	R=0.247 p=0.465	R=0.338 p=0.512

## APPENDIX G – TRENDS OF ONSD

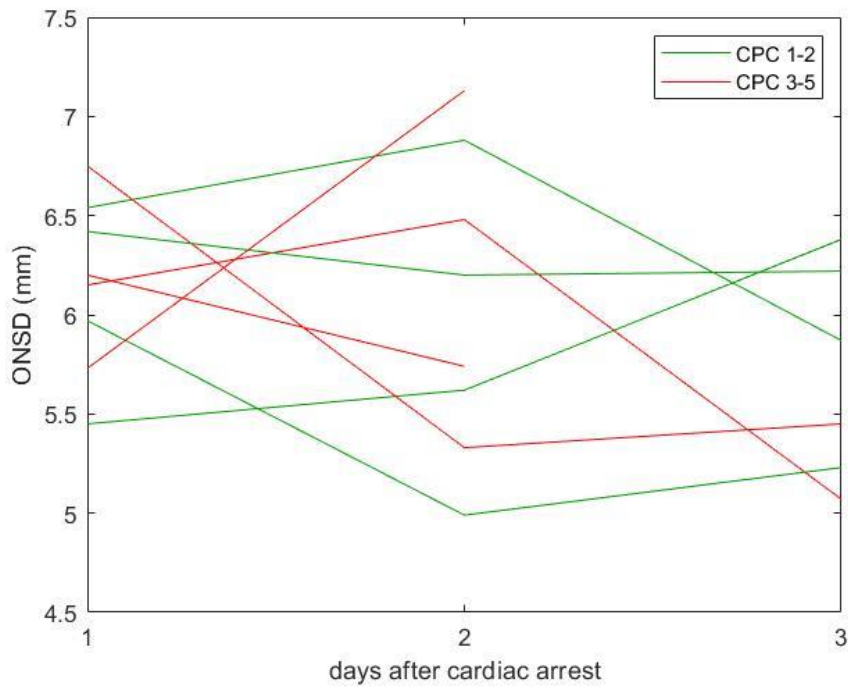


FIGURE G.1 CHANGES OF ONSD DURING THE FIRST THREE DAYS AFTER RESUSCITATION FOR PATIENTS WITH GOOD (GREEN) AND POOR (RED) NEUROLOGICAL OUTCOME.